Quaternary Science Reviews 168 (2017) 101–122

Contents lists available at ScienceDirect

Quaternary Science Reviews

journal homepage: www.elsevier.com/locate/quascirev

A full holocene tephrochronology for the Kamchatsky Peninsula region: Applications from Kamchatka to North America

Vera Ponomareva [a, *], Maxim Portnyagin [b, c], I. Florin Pendea [d], Egor Zelenin [e], Joanne Bourgeois [f], Tatiana Pinegina [a], Andrey Kozhurin [a, e]

[a] Institute of Volcanology and Seismology, Piip Boulevard 9, Petropavlovsk-Kamchatsky 683006, Russia
[b] GEOMAR Helmholtz Center for Ocean Research Kiel, Wischhofstrasse 1-3, 24148 Kiel, Germany
[c] V.I. Vernadsky Institute of Geochemistry and Analytical Chemistry, Kosygin St. 19, Moscow 119991, Russia
[d] Lakehead University, Sustainability Sciences Department, 500 University Avenue, Orillia, ON L3V0B9, Canada
[e] Geological Institute, Pyzhevsky Lane 7, Moscow, 119017, Russia
[f] Department of Earth and Space Sciences, University of Washington, 4000 15th Avenue NE, Seattle, WA 98195-1310, USA

ARTICLE INFO

Article history:
Received 30 October 2016
Received in revised form
15 March 2017
Accepted 28 April 2017
Available online 19 May 2017

Keywords:
Holocene
Paleogeography
Tephrochronology
Northern Pacific
Kamchatka
Data analysis
Volcanic glass chemistry
Age modeling

ABSTRACT

Geochemically fingerprinted widespread tephra layers serve as excellent marker horizons which can directly link and synchronize disparate sedimentary archives and be used for dating various deposits related to climate shifts, faulting events, tsunami, and human occupation. In addition, tephras represent records of explosive volcanic activity and permit assessment of regional ashfall hazard. In this paper we report a detailed Holocene tephrochronological model developed for the Kamchatsky Peninsula region of eastern Kamchatka (NW Pacific) based on ~2800 new electron microprobe analyses of single glass shards from tephra samples collected in the area as well as on previously published data. Tephra ages are modeled based on a compilation of 223 ^{14}C dates, including published dates for Shiveluch proximal tephra sequence and regional marker tephras; new AMS ^{14}C dates; and modeled calibrated ages from the Krutoberegovo key site. The main source volcanoes for tephra in the region are Shiveluch and Kliuchevskoi located 60–100 km to the west. In addition, local tephra sequences contain two tephras from the Plosky volcanic massif and three regional marker tephras from Ksudach and Avachinsky volcanoes located in the Eastern volcanic front of Kamchatka. This tephrochronological framework contributes to the combined history of environmental change, tectonic events, and volcanic impact in the study area and farther afield. This study is another step in the construction of the Kamchatka-wide Holocene tephrochronological framework under the same methodological umbrella. Our dataset provides a research reference for tephra and cryptotephra studies in the northwest Pacific, the Bering Sea, and North America.

1. Introduction

Tephra layers are widely used for correlation and dating of various deposits and landforms and for the synchronization of disparate paleoenvironmental archives. These applications are in high demand in paleoclimatology, paleoseismology, archaeology, and other Quaternary science disciplines (e.g., Alloway et al., 2007; Lowe, 2011). Regions located within 100 km of active volcanoes often host sequences of visible tephra layers which permit the construction of detailed tephrochronological frameworks for dating deposits and landforms formed by various geological events (e.g., Braitseva et al., 1997; Shane, 2005; Fontijn et al., 2016; Nakamura, 2016). For instance, in eastern Kamchatka deposits left by catastrophic events such as tsunami, co-seismic subsidence, liquefaction, and faulting form distinct silt, sand and debris layers or wedges sandwiched between tephra layers which can be differentiated by thickness, color, grain size, stratification, grading and physical properties (Figs. 1–3). In paleotsunami research, for example, tephra layers have been a major tool for correlation between and among sites along the Japan-Kuril-Kamchatka subduction zone (e.g., Bourgeois et al., 2006; Sawai et al., 2009; MacInnes

* Corresponding author.
E-mail addresses: vera.ponomareva1@gmail.com (V. Ponomareva), mportnyagin@geomar.de (M. Portnyagin), ifpendea@lakeheadu.ca (I.F. Pendea), egorzelenin@mail.ru (E. Zelenin), jbourgeo@u.washington.edu (J. Bourgeois).

http://dx.doi.org/10.1016/j.quascirev.2017.04.031
0277-3791/

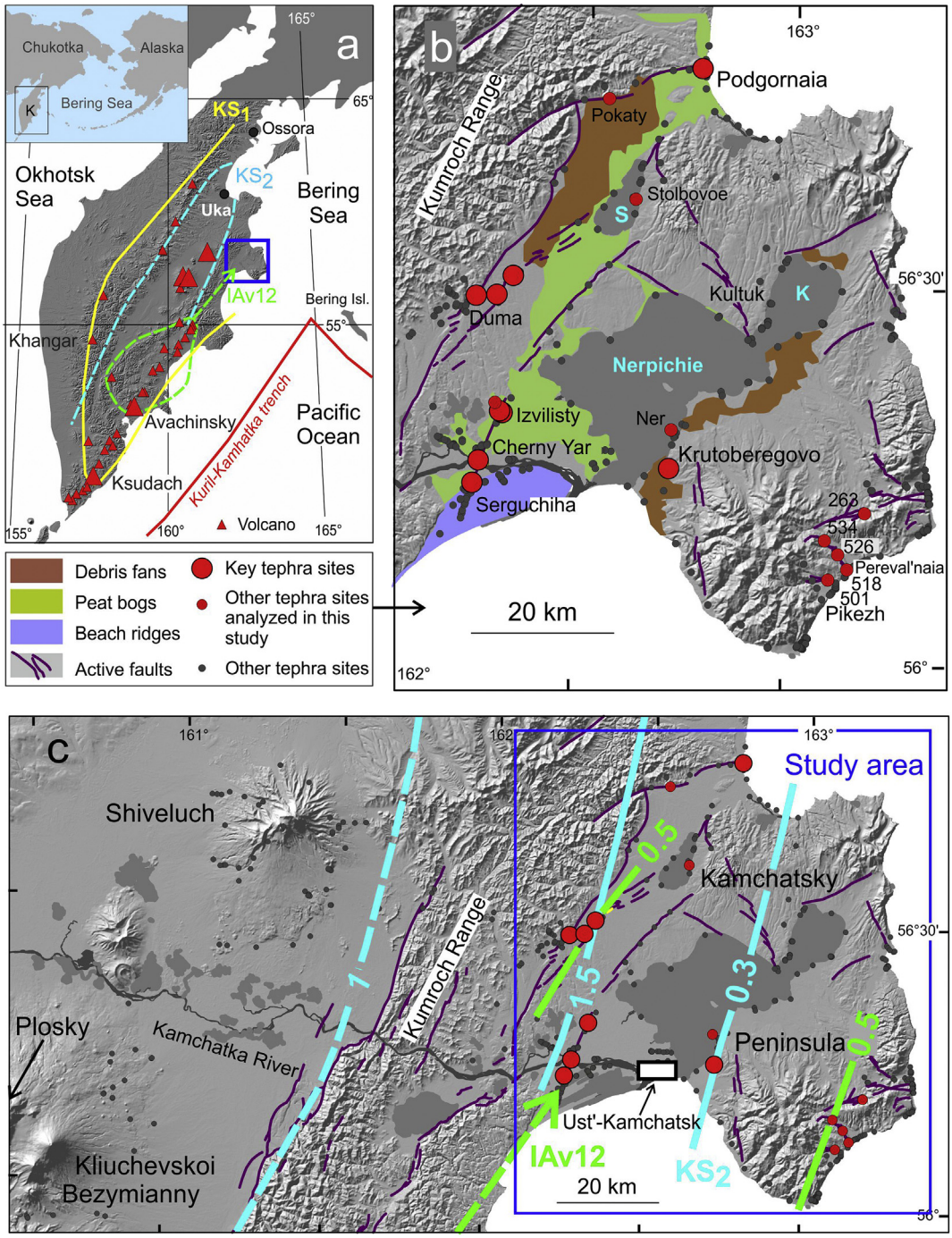

Fig. 1. Locations of the study area (dark blue frames on **a** and **c**), volcanoes, and main tephra sites shown on SRTM global digital elevation model (spatial resolution is approx. 90 m; data available from the U.S. Geological Survey). Inset in **a** shows position of the Kamchatka Peninsula (K). **a** – position of the study area relative to the Kamchatka-Aleutian junction. Holocene volcanoes are shown with red triangles, larger triangles show source volcanoes for tephras in the study area. Volcanoes mentioned in the text are labeled here and in **b** and **c**. Volcanic chain along the eastern coast of Kamchatka forms the Eastern Volcanic Front. Dispersal area (1 cm outline) of the main regional tephras known to have reached the study area is shown with lines and labels of matching colors: KS_1 and KS_2 according to Braitseva et al. (1997) refined after Kyle et al. (2011) and Plunkett et al. (2015); IAv12 (AV_4) – outline according to Braitseva et al. (1998) with an arrow to the Cherny Yar site where this tephra was mentioned by Bazanova et al. (2005). **b** – detailed map for the study area showing major morphological features and active faults (Pinegina et al., 2014), and research sites; legend for **b** is located left of the map. Lakes are in dark-gray and labeled with blue: S – Stolbovoe Lake, K – Kultuchnoe Lake; **c** – position of study area relative to closest active volcanoes: Shiveluch, Plosky, Kliuchevskoi, and Bezymianny. Location of Ust'-Kamchatsk village is labeled. Newly determined positions of isopachs for IAv12 and KS_2 tephras are shown in solid lines, thickness in cm. Other symbols as in **a** and **b**. (For interpretation of the references to colour in this figure legend, the reader is referred to the web version of this article.)

et al., 2016); tsunami deposits themselves are often lacking unique features and therefore cannot be differentiated on their own (Bourgeois et al., 2006). Tephra layers have also been used to determine landslide and turbidity-current frequencies, which may be correlated with paleoseismic events (e.g., Adams, 1990; Moernaut et al., 2014; Pouderoux et al., 2014). Paleoseismological studies of active faults use tephra layers to date faulting events and correlate them over the fault system, and also to evaluate the rate of

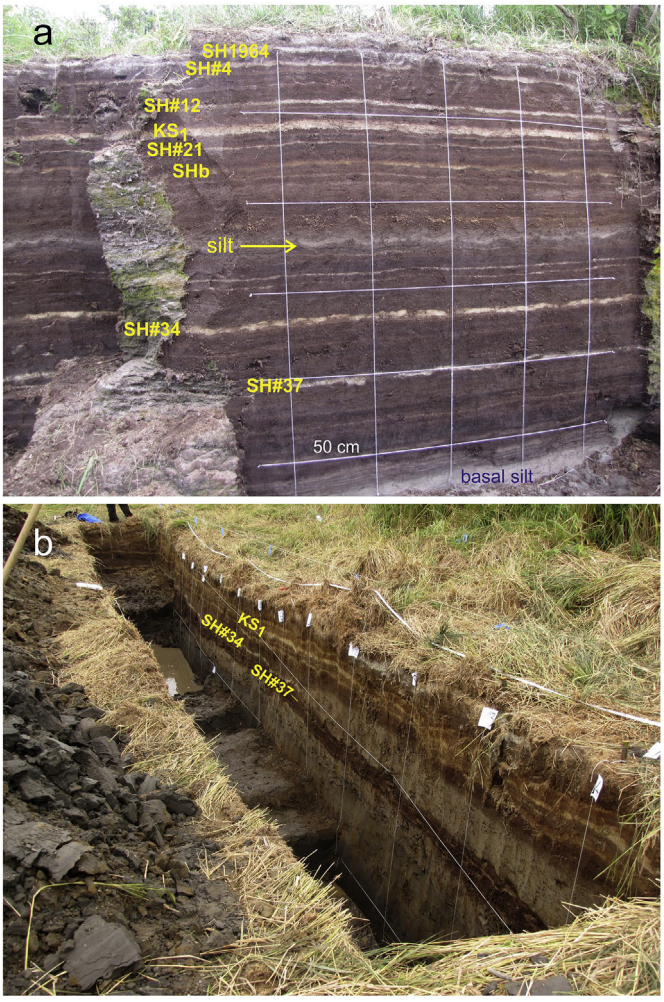

Fig. 2. Photos of key tephra sequences in the study area: **a** – tephra layers in Cherny Yar ("Black bluff") peat section, originally studied by Pevzner et al. (1998). Tephra codes as in Table 2. Each grid cell is 50 × 50 cm. **b** – One of the Izvilisty trenches. Silt wedge produced by liquefaction intrudes the tephra-peat sequence directly above SH#34 tephra, which permits dating of the faulting event at ~4.7 ka (Pinegina et al., 2012).

tectonic deformation (e.g., Townsend, 1998; Turner et al., 2008; Kozhurin et al., 2006, 2014; Pinegina et al., 2014; Sherrod et al., 2016). Tephrochronology also helps validate paleogeographical reconstructions and identify the age and nature of landforms once suitable for human settlement (e.g. dry versus flooded areas). In addition, these reconstructions suggest how much archaeological evidence may have been reworked or removed by erosional processes (e.g., Pinegina et al., 2013a; MacInnes et al., 2014; Schmid et al., 2016). Studies of tephra sequences and correlations of the tephra layers between disparate sites permit reconstruction of the eruptive histories on a local and regional scale (e.g., Kutterolf et al., 2008a; Óladóttir et al., 2011; Fontijn et al., 2014) and assessment of explosive eruptions magnitudes (e.g., Kutterolf et al., 2008b; Ponomareva et al., 2013a, b; Schindlbeck et al., 2016).

The Kamchatka Peninsula (Fig. 1a) hosts more than 37 recently active large volcanic centers and a few hundred monogenetic vents comprising the northwestern segment of the Pacific Ring of Fire. Kamchatka tephra layers provide chronological control for deposits and events over large areas, which is critical for many studies (e.g., Hulse et al., 2011; Kozhurin et al., 2014; Pinegina et al., 2012, 2013b, 2014; Plunkett et al., 2015; Pendea et al., 2016), but geochemical characterization of Kamchatka volcanic glasses to strengthen correlations on a regional scale is still in a developing phase. Geochemical characterization of volcanic glass has become the most common practice for correlations of tephra layers in various volcanic regions (e.g. Larsen, 1981; Shane, 2000; Gehrels et al., 2006; Lawson et al., 2012; Fontijn et al., 2014, 2016; Davies et al., 2016; Gudmundsdóttir et al., 2016). In the Kamchatka volcanic arc, however, the Holocene tephrochronological framework until recently has been based mainly on direct tracing of tephra layers, bulk composition of tephra, and radiocarbon dates (e.g., Braitseva et al., 1995, 1996, 1997, 1998; Pevzner et al., 1998, 2006, Pevzner, 2010; Bazanova et al., 2005) with only few papers providing data on glass compositions (Dirksen et al., 2011; Kyle et al., 2011; Ponomareva et al., 2012, 2013a,b; 2015; Plunkett et al., 2015).

In this paper we present a detailed Holocene tephrochronological framework for the Kamchatsky Peninsula – a promontory in northeastern Kamchatka situated between the Pacific Ocean and Bering Sea – based on ~2800 electron microprobe glass analyses from 186 tephra samples collected from excavations, natural outcrops and sediment cores. First, we establish tephra stratigraphy based on geochemical fingerprinting of tephra layers from six key sequences. Then we analyze 48 unknown tephra samples collected from several deformed tephra sequences unearthed in paleoseismological trenches and cores, as well as from an archaeological test pit, and subsequently match them to a developed stratigraphy in order to test the applicability of our results. This study uses the same analytical methods as in our previous works (Ponomareva et al., 2012, 2013a, b, 2015), and we combine previously obtained radiocarbon dates with new ones to better constrain tephra ages. The resulting high-resolution tephrochronological framework will help decipher the temporal and spatial complexity of archaeological records, seismic events, volcanic eruptions, and environmental change in this highly dynamic area. In addition, identification of tephra layers contributes to a better understanding of regional eruptive histories, magnitudes of past eruptions, and risk from volcanic hazards.

2. Physiography and tephra deposits of the study area

The Kamchatsky Peninsula is the northernmost of three distinct promontories at the eastern coast of the Kamchatka Peninsula (Fig. 1). It is situated at the northern terminus of the Kuril-Kamchatka subduction zone and is a locus of collision between the Aleutian island arc and Kamchatka (e.g., Geist and Scholl, 1994; Pedoja et al., 2013; Kozhurin et al., 2014). Because of this tectonic setting, the area has experienced a suite of dramatic natural events and processes including strong subduction-related earthquakes, destructive tsunamis, co-seismic subsidence and uplift, crustal faulting, and volcanic ash-falls (Pevzner et al., 1998; Bourgeois et al., 2006; Pinegina et al., 2013b, 2014; Kozhurin et al., 2014; Pendea et al., 2016). These natural processes have dramatically and repetitively altered the topography, drainage patterns, and environment of the area (Pedoja et al., 2013; Pendea et al., 2017). As such they will have affected humans living on Kamchatka, for which there is an archaeological record spanning the entire Holocene (Goebel et al., 2003, 2010).

The study area consists of two contrasting parts: mountainous terrain in the east and a large stretch of lowland to the west, flanked in turn by the Kumroch Range (Fig. 1); the lowland hosts three large lakes (Stolbovoe, Nerpichie, and Kultuchnoe) and vast peatlands. The closest active volcanoes are Shiveluch (≥60 km to the west) and Kliuchevskoi (≥100 km to southwest) (Fig. 1c). Other Kliuchevskoi group volcanoes active during the Holocene are Bezymianny, Plosky (Fig. 1c), and the Tolbachik monogenetic field (~30 km southwest of Bezymianny). Ash plumes from these

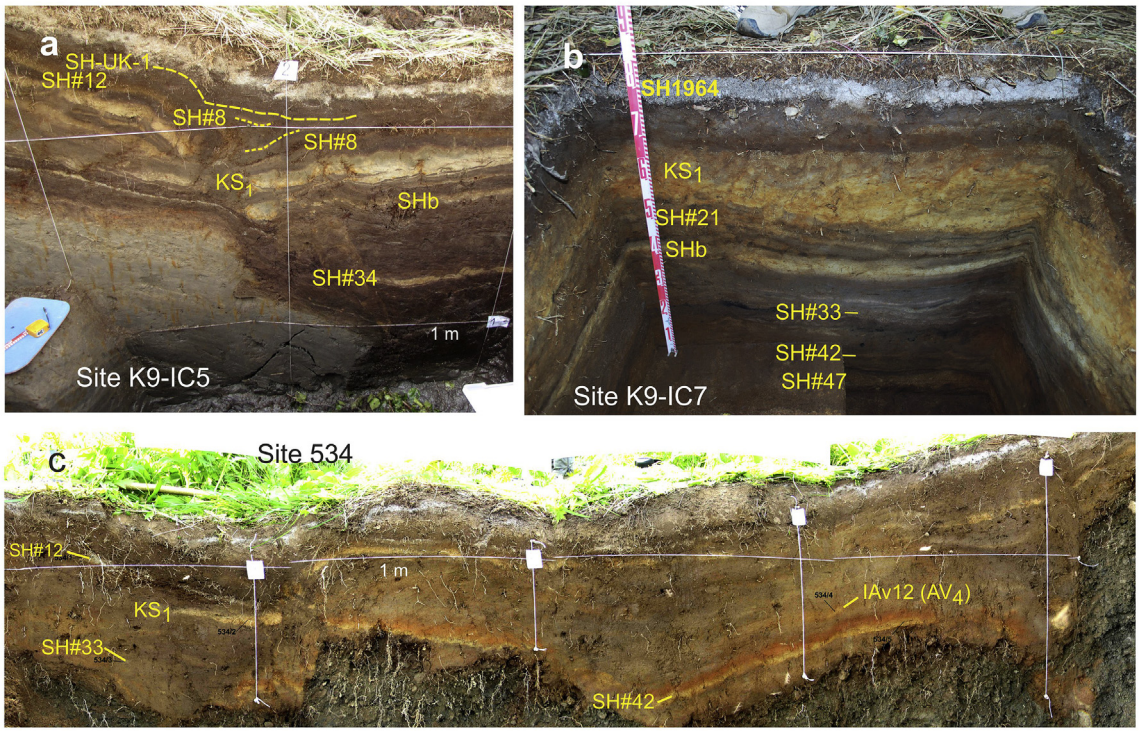

Fig. 3. Photos of disturbed tephra sequences: **a** – Izvilisty paleoseismological trench. Timing of the most recent faulting event is defined by broken (SH#8) and overlying non-disturbed (SH-UK-1) tephra layers. **b** – archaeological test pit at the Izvilisty site. Archaeological layer(s) marked by charcoal and soils at the bottom of the pit destroyed all the tephras between SH#33 and SH#47 except for SH#42, which is found as long lenses within the archaeological layer (Hulse et al., 2011). **c** – paleoseismological trench 534 through soil-tephra sequence in Perevalnaya site where broken tephra layers were treated as unknowns (see text).

volcanoes have repeatedly reached distances of >100 km from the source (Fedotov, 1984; Fedotov and Masurenkov, 1991; Ponomareva et al., 2013a, 2015). Other active volcanoes are located in the Eastern volcanic front and Sredinny Range, all ≥170 km from the study area (Fig. 1a).

A large part of the study area is covered with thick Holocene peat which is among the best archives to preserve tephra layers as visible horizons (e.g., Fig. 2a). Accumulation rates for the peat in the study area vary between 0.4 and 0.7 mm/yr (Pevzner et al., 1998; Pendea et al., 2017), which ensures fast burial of tephra and thus a clear differentiation of distinct tephra layers. In addition, peat provides material for radiocarbon dating. Most peat in the study area is younger than 7.8 ka, but older peat (~10.2 ka – present) was excavated from a former kettle lake near Krutoberegovo village (Fig. 1; Pendea et al., 2017). Beyond the peatland, tephra horizons are interlayered with eolian sandy loams and paleosols forming continuous sequences from ~12 ka to present. These sequences overlie silts, sands or coarse gravels likely related to the Last Glacial Maximum (LGM).

Tephra layers in the study area differ in grain size (from silts to small lapilli), thickness (from a few mm to 10 cm), color, texture, and geochemistry, with the maximum number of tephra layers in a single section reaching 41. Unique sequences of these tephra layers allow tracing not only of individual layers, but also of stratigraphically ordered tephra packages. Nearby Shiveluch volcano is the source for most of the tephra deposits (Pevzner et al., 1998; Figs. 1c and 2), which are dominantly andesitic in bulk composition and generally difficult to distinguish geochemically because they are compositionally similar and contain only small pockets of residual glass in a further crystalline groundmass (Plunkett et al., 2015; Ponomareva et al., 2015). Recent detailed study of Shiveluch proximal tephra, however, has shown that several andesitic and two basalt/basaltic andesite tephras have unique glass compositions (Ponomareva et al., 2015). In addition, glasses from Shiveluch andesitic tephras exhibit temporal variations in SiO_2 and some other oxides, which facilitates geochemical correlation to their distal counterparts.

Tephra layers around the Kamchatsky Peninsula area were first mentioned during reconnaissance paleotsunami studies (Melekestsev et al., 1994). Mapped dispersal areas for three regional tephra markers (KS_1 from Ksudach, AV_4 [new label is IAv12] from Avachinsky, and KHG from Khangar volcanoes, Fig. 1a) suggested that these layers should have been deposited in the study area (Braitseva et al., 1996, 1997). These and other tephras were first identified via chemical analyses of bulk tephra samples, radiocarbon dates on bulk organic samples, and extrapolation of tephra thickness data. Later studies of the Cherny Yar peat outcrop (Figs. 1b and 2; Pevzner et al., 1998) allowed documentation of 34 individual tephra layers, deposited during the last ~6.8 ka. These studies confirmed the presence of KS_1 and IAv12 (AV_4) layers in the area based on ^{14}C dates on bulk peat. They also demonstrated that the KHG layer pinches out eastward along the profile from Shiveluch volcano towards Cherny Yar so it is not present in the Kamchatsky Peninsula. Twenty eight tephra layers in Cherny Yar were attributed to Shiveluch volcano based on direct tracing of tephra layers from the volcano to this site and on ^{14}C dates of bulk peat. In addition, several dark-gray cindery layers were tentatively ascribed to basaltic Kliuchevskoi volcano. Published dispersal areas for a few Shiveluch marker tephras also suggested presence of some of these tephras in the Kamchatsky Peninsula area (Braitseva et al., 1997; Ponomareva et al., 2007; Kyle et al., 2011). In these studies some of the Shiveluch tephras were labeled with their non-calibrated ^{14}C age averaged from several dates and rounded to the nearest hundred years (e.g., SH2800).

The first electron microprobe data on glass from selected tephra samples in the study area were obtained by Bourgeois et al. (2006) for the Podgornaia site (Fig. 1b). Kyle et al. (2011) provided more glass data for six tephra layers from the same section including KS_1 from distal Ksudach volcano (southern Kamchatka, Fig. 1a). In addition, Kyle et al. (2011) identified another regional tephra from Ksudach (KS_2) at the Uka site ~170 km NNW from our study area (Fig. 1a) based on similarity of the Uka tephra glass composition to that from the known KS_2 sites. Plunkett et al. (2015) identified both KS_1 and KS_2 tephra layers ~300 km farther north in lake deposits near Ossora village (Fig. 1a). Recent studies have allowed Mackay et al. (2016) and Pyne-O'Donnell (pers. comm.) to identify KS_1 and KS_2 cryptotephra deposits in eastern Canada. Additionally, two early Holocene marker tephras (PL1 and PL2) from the Plosky volcanic center have been identified, geochemically fingerprinted, mapped and dated in the study area (Ponomareva et al., 2013a). At least two different early Holocene Shiveluch tephras were found in marine cores ~450 km east of the Kamchatsky Peninsula, which suggested they should be present in our study area as well (Ponomareva et al., 2015).

Some of the tephra layers in the area have already been used for dating tsunami deposits (Bourgeois et al., 2006), marine terraces (Pinegina et al., 2013b), faulting events (Pinegina et al., 2014; Kozhurin et al., 2014), and archaeological horizons (Hulse et al., 2011; Pendea et al., 2016). However, to date there is no systematic stratigraphy available, and there is a lack of well-constrained ages and chemical composition of the marker tephra horizons in the area.

3. Methods

3.1. Stratigraphic studies

During our studies we have measured ~300 Holocene sections in the area from Kliuchevskoi and Shiveluch volcanoes in the west to the study area in the east (Fig. 1c) (Pevzner et al., 1998; Ponomareva et al., 2013a, 2015). Data from these sections help us directly trace individual tephra layers throughout the whole region. In four major localities – Krutoberegovo, Izvilisty, Duma, and Serguchiha (Fig. 1) – most visible tephra layers were analyzed for glass compositions (Fig. 4a–d; Electronic Supplement Tables 1 and 2). The Krutoberegovo and Serguchiha sections are represented by one excavation/core, while the other two localities each comprise several closely spaced individual excavations combined in two summary sections. In addition, we have sampled selected tephras in the previously described Podgornaia and Cherny Yar localities, from several paleoseismological and archaeological excavations, and from Nerpichie Lake sediments (Fig. 1b). Further on tephras are labeled according to Braitseva et al. (1997, 1998) and Ponomareva et al. (2013a, 2015). Shiveluch tephras are labeled SH followed with the number of the unit according to the proximal nomenclature (Ponomareva et al., 2015); old labels for several regional marker tephras are provided in brackets and follow Braitseva et al. (1997). Newly identified tephras from Shiveluch and Kliuchevskoi, which occur in more than one section, are labeled SH-UK-1 – 4 and KL-UK-1 – 3, respectively.

The **Krutoberegovo** site JB112 (N56.25334°, E162.71386°) presents the temporally longest (>14 ka), high-resolution section in the area and consists of a 4-m-deep excavation extended with a 3-m-long core taken from the bottom of this excavation (Pendea et al., 2017). The upper 680 cm are peat, and the lower 20 cm are lake deposits (Fig. 4a–d). The **Duma** section (Fig. 1) is based mostly on a 3.7-m-deep peat excavation (site YK2008-04; N56.4990°, E162.3235°; bottom at ~8.8 ka) supplemented with three closely spaced sections (YK20018-01 – 03) that feature soil-pyroclastic sequences of older age (up to ~12 ka). The **Izvilisty** section (Fig. 1b) is based on a 1.3-m-deep peat excavation (site K9-IC1; N56.3199°, E162.3150°) supplemented by two additional peat excavations and three paleoseismological trenches with the oldest peat at ~5.8 ka. The **Serguchiha** site 619-2012 (N56.22527°, E162.24977) (Fig. 1b) is a 2.5-m-deep peat excavation with a bottom at ~5.5 ka.

We resampled selected tephra layers in earlier studied **Podgornaia** and **Cherny Yar** sections (Fig. 1). Our new 2.5-m-long peat core labeled AL (N56.7859°, E162.7750°) was taken ~500 m southwest from the **Podgornaia** site (labeled 125/99-04 in Bourgeois et al., 2006). The **Cherny Yar** site is a peat outcrop ~1 km long along the Kamchatka River, where we measured sections every ~100–150 m to compile a summary section (Figs. 1b, 2 and 4a-d). The section measured by Pevzner et al. (1998) is located in the eastern part of the outcrop.

3.2. Radiocarbon dating and age estimates for tephra layers

Most of the earlier studies (e.g., Pevzner et al., 1998; Bourgeois et al., 2006) report radiocarbon ages based on samples of bulk peat. However, dates on bulk peat can yield apparent younger ages because of root penetration (e.g., Zaretskaia et al., 2001; Bourgeois et al., 2006). The first date on plant macrofossils in the area (underneath KS_1 regional tephra) was reported by Pinegina et al. (2013b). We obtained a set of 21 new AMS ^{14}C dates for two of our key peat sections – Krutoberegovo and Izvilisty (Pendea et al., 2016). Sixteen dates from the Krutoberegovo site have been used to construct an age-depth model for this section (Pendea et al., 2017); details on the stratigraphy of Izvilisty samples are shown in Table 1. The dates from the Shiveluch proximal tephra sequence were reported by Ponomareva et al. (2015).

To provide a comprehensive tephrochronologic tool for the study area we constructed a regional synthesis of major tephra layers (Table 2) following the method proposed by Blockley et al. (2008). Age probability distributions of individual tephra layers in a composite tephrostratigraphy were modeled using Bayesian statistics in OxCal 4.2 (Bronk Ramsey, 2009a,b) with the IntCal13 calibration curve (Reimer et al., 2013). The new model uses all the ^{14}C dates included into the Shiveluch proximal model (Ponomareva et al., 2015) plus new dates from the study area (Pinegina et al., 2013b; Pendea et al., 2016) as well as dates for regional marker tephra layers obtained elsewhere (Braitseva et al., 1997, 1998). Correlation of these sections was constrained by stratigraphic position and geochemical data for the tephras, as discussed below. In addition, for tephras present in the Krutoberegovo site but not dated elsewhere we included their modeled calibrated ages with known uncertainties from the age-depth model by Pendea et al. (2017) (Electronic Supplement Text A.1). This approach permitted age estimates for most tephra layers in the study area and also the refinement of ages for Shiveluch tephras in the proximal summary section and for regional marker tephras (e.g., Blockley et al., 2008; Electronic Supplement Table A.1, last sheet). Modeled ages of the marker tephras are reported in Table 2 and supplementary tables A.1 and A.2. Previous age estimates, where available, are provided in the Electronic Supplement Table A.1 (sheet 8). We report ages in calibrated years before 1950 CE. For loose (approximate) dates we use designation ka (calibrated kyr before 1950 CE; e.g., "our record spans ~14 ka").

3.3. Electron microprobe analysis

We have analyzed volcanic glass from 186 tephra samples collected in 24 sections in the study area and from 25 reference samples of proximal tephra of four volcanoes (Electronic Supplement Table A.2). Analyses were performed at GEOMAR

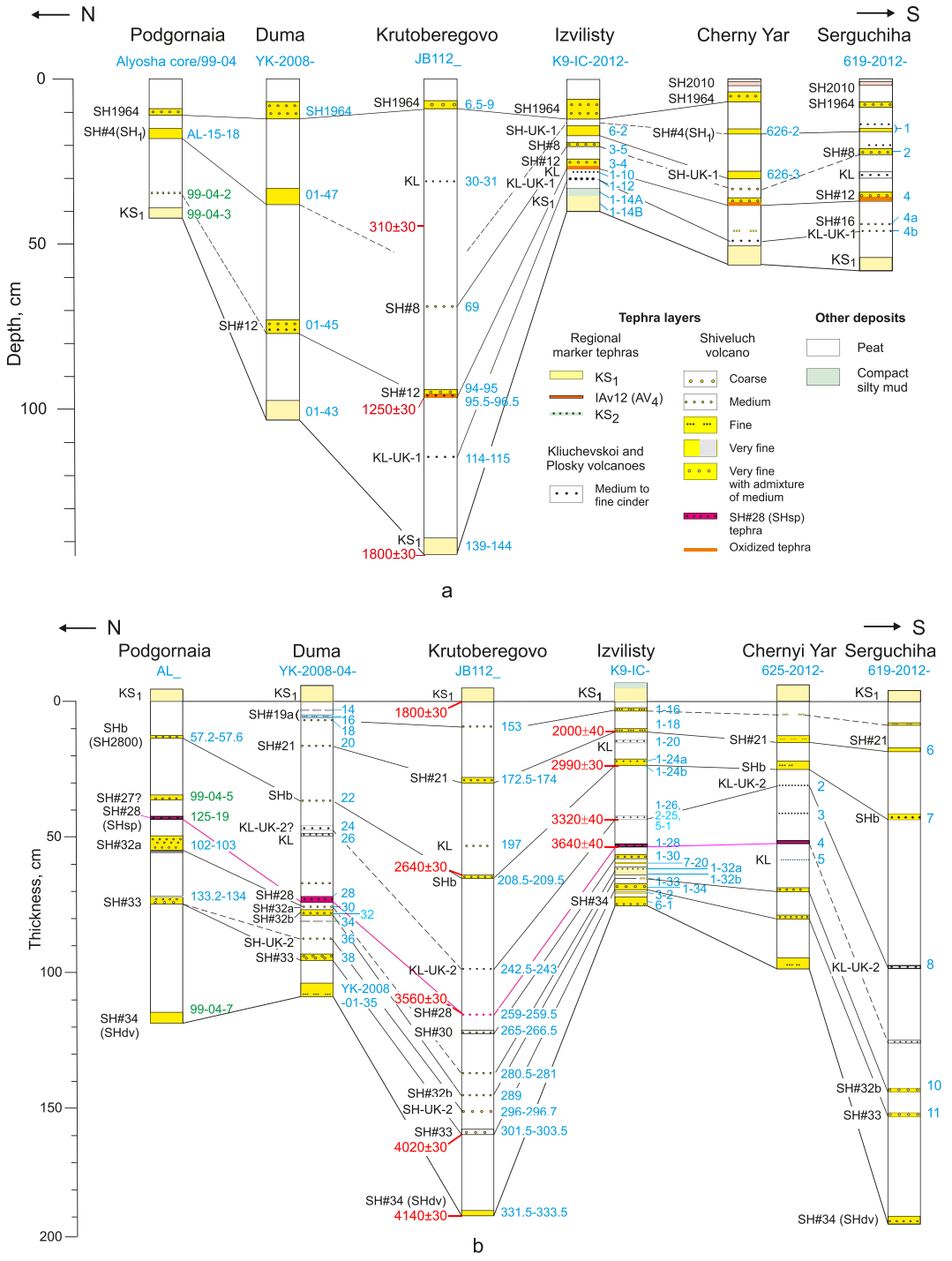

Fig. 4. a-d Schematic tephra sections in the key study sites (Fig. 1) split into stratigraphic intervals between major marker tephras. Identified tephras are labeled to the left of the columns after Braitseva et al. (1997, 1998) and Ponomareva et al. (2013a, 2015). Shiveluch tephras are labeled SH followed with the number of the unit according to the proximal nomenclature (Ponomareva et al., 2015); old labels for several regional marker tephras are provided in brackets and follow Braitseva et al. (1997). KS_1 and KS_2 – tephras from Ksudach volcano (South Kamchatka); KL – tephra from Kliuchevskoi volcano; IAv12 (AV_4) – tephra from Avachinsky volcano; PL1 and PL2 – tephras from Plosky volcanic center. Newly identified tephras from Shiveluch and Kliuchevskoi, which occur in more than one section, are labeled SH-UK-1 – 4; and KL-UK-1 – 3, respectively. Tephra samples analyzed in this study are shown in blue to the right of the columns. Several samples from Kyle et al. (2011) and Bourgeois et al. (2006) are shown in green. New AMS dates on macrofossils and bulk sediment for Krutoberegovo and Izvilisty sites (Pendea et al., 2016, 2017; Table 1) are shown in red to the left of the sections; selected published dates (Pevzner et al., 1998; Bourgeois et al., 2006) are shown in purple. Dates obtained on the successive alkaline extractions from the same sample are shown in boxes (see Braitseva et al., 1993; for method description). (For interpretation of the references to colour in this figure legend, the reader is referred to the web version of this article.)

(Kiel, Germany) between 2009 and 2015 following the same protocol as in Ponomareva et al. (2012, 2013a,b, 2015). Volcanic glass was analyzed using JEOL JXA 8200 electron microprobe equipped with five wavelength dispersive spectrometers including 3 high-sensitivity ones (2 PETH and TAPH). The analytical conditions for glasses were 15 kV accelerating voltage, 6 nA current and 5 μm

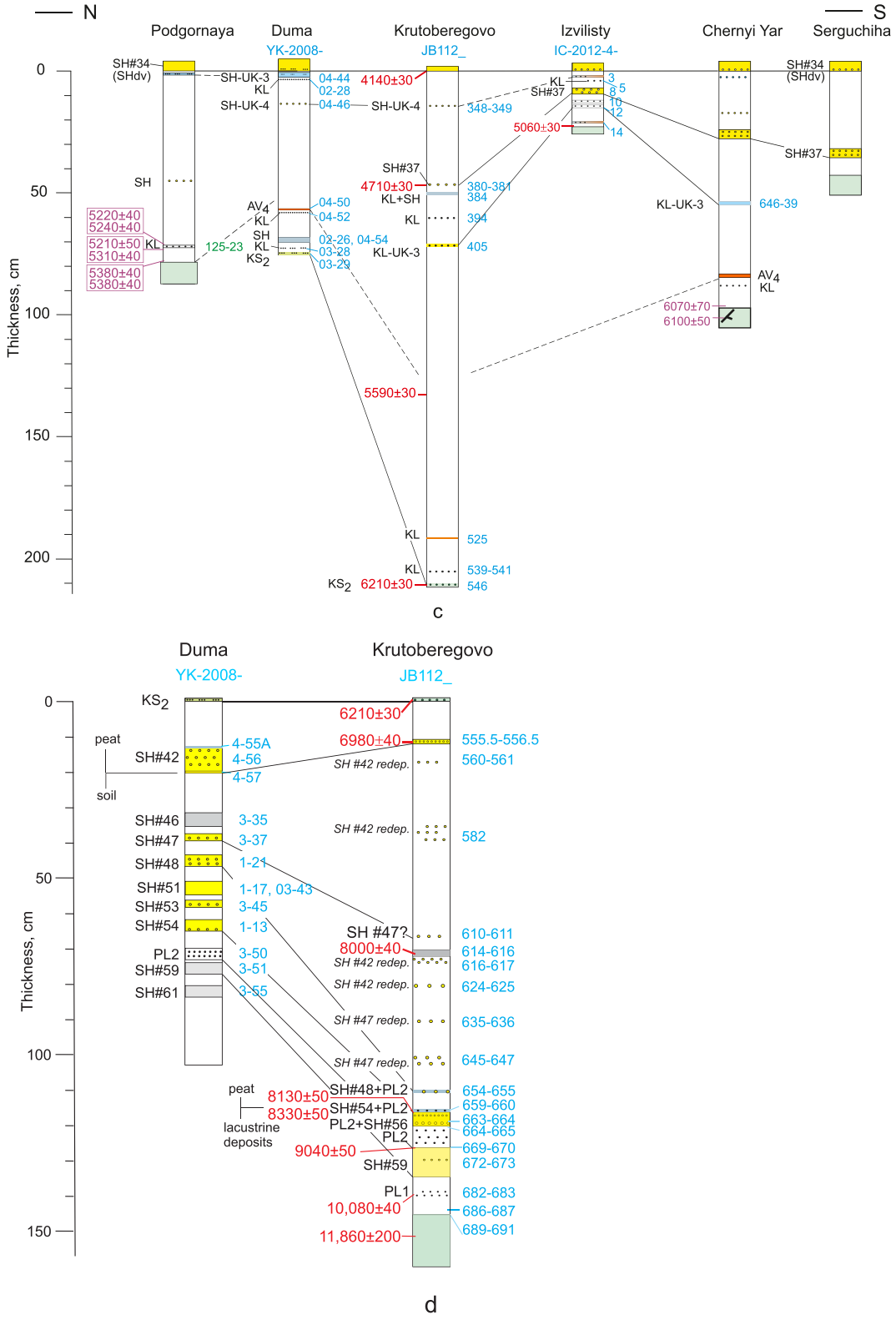

Fig. 4. (*continued*).

electron beam size. Details of the analytical technique are given in Supplementary Text A.2 and Electronic Supplement Tables A.3 and A.4. This file contains comprehensive information concerning the analytical conditions, reference materials, long-term precision and reproducibility of microprobe analyses, uncertainty of single-point analysis (interactive table) and details of data reduction, which are applied to all data obtained since 2008, including this study. Accuracy and precision of the microprobe data is illustrated in

Table 1
Radiocarbon dates for Izvilisty peat section.

Stratigraphic position	Depth from surface (cm)	Sample description	Lab ID	^{14}C date
Immediately below tephra K9-IC1-18 SH#21 (SH_5)	48	Stems epidermis, seeds fragments	OS-80101	2000 ± 40
Immediately below tephra K9-IC1-24 SHb (SH2800)	60	Briales stems; Carex epidermis	OS-80031	2990 ± 30
Immediately below tephra K9-IC1-26 (KL-UK-1)	80	Seeds fragments	OS-80098	3320 ± 40
Immediately below tephra K9-IC1-28 SH#28 (SHsp)	89	Epidermis of the leaf vagina; Najas seed	OS-80038	3640 ± 40
Below tephra K9-IC4-14 and on the top of silt layer	129	Organic sediment	OS-80032	5060 ± 30

Notes: All the dates were obtained at the National Ocean Sciences AMS Facility. The dates were published by Pendea et al. (2016). Details on stratigraphy of the dated samples and material used for dating are provided in this table.

Table 2
Major tephra markers in the Kamchatsky Peninsula and Stolbovaia depression.

Tephra code	Tephra source	Thickness (cm)	Ages (2σ intervals; cal a BP)	Weighted mean (cal a BP)	Description/grain-size
SH2010	Shiveluch	1–2	–	−60 (2010 CE)	Dull-pinkish-gray fine ash
SH1964	Shiveluch	2–6	–	−14 (1964 CE)	Salt-and-pepper medium sandy ash
SH#4 (SH_1)	Shiveluch	0–5	305–317	311	White fine to very fine ash
SH#8	Shiveluch	0–3	960–1155	1049	White fine to medium sandy ash
SH#12 (SH1450)	Shiveluch	1–4	1311–1408	1356	Reverse graded ochre-gray salt-and-pepper coarse sandy ash
KL-UK-1	Kliuchevskoi	0–1	1339–1625	1469	Black fine ash
KS_1	Ksudach	3–7	1590–1705	1651	Pale-yellow with grayish top reverse-graded fine to very fine ash
SH#19a	Shiveluch	0–1	1649–1899	1773	Light-yellow very fine to fine ash, in places splits in two or three layers
SH#21 (SH_5)	Shiveluch	0–2	1885–1984	1934	Pale-yellow very fine to fine ash
SHb (SH2800)	Shiveluch	1–2	2794–3013	2903	Bright greenish-yellow very fine to fine ash
KL-UK-2	Kliuchevskoi	0.5–1	3010–3590	3329	Black fine ash
SH#28 (SHsp)	Shiveluch	0.5–1	3845–3986	3912	Shiny gray – dark-gray fine ash
SH#30	Shiveluch	0–2	3900–4120	4006	Salt-and-pepper medium to coarse sandy ash
SH#33	Shiveluch	1–2	4305–4510	4414	Light-tan pumice sandy ash with small lapilli
SH#34 (SHdv)	Shiveluch	2–4	4600–4817	4712	Normal-graded pale-yellow ash: very fine ash at the top to fine ash at the bottom.
SH#37	Shiveluch	1–4	5421–5626	5522	Salt-and-pepper medium sandy ash
KL-UK-3	Kliuchevskoi	0–1	5586–6096	5829	Dark-gray fine ash
IAv12 (AV_4)	Avachinsky	0–0.5	6220–6375	6281	Bright-yellow very fine ash
KS_2	Ksudach	0.3–0.5	6693–6877	6786	Greenish-tan fine ash
SH#42	Shiveluch	1–5	7601–7720	7665	Tan salt-and-pepper medium sandy ash
SH#47	Shiveluch	1–2	8362–8750	8521	Tan medium to coarse sandy ash
SH#48	Shiveluch	1–3	8551–9046	8805	Coarse sandy to very fine ash
SH#51	Shiveluch	2–4	9136–9595	9375	Light-yellow fine ash
SH#53	Shiveluch	1–2	9391–9900	9640	Gray salt-and-pepper medium sandy ash
SH#54	Shiveluch	1–3	9489–10016	9731	Normal-graded fine to medium sandy ash
PL2	Plosky	3–6	9970–10292	10211	Dark-brownish-gray cindery coarse sandy ash
SH#59	Shiveluch	3	10456–11042	10737	Dull-gray-tan fine ash
PL1	Plosky	1	10615–11457	10958	Dark-brownish cindery fine ash
SH#61	Shiveluch	3	10865–11582	11120	Dull-gray fine ash

Note: Tephra layers are listed in stratigraphic order from top to bottom. Tephra layers uniquely identified based on their appearance and/or glass composition are highlighted in pale yellow. Identified tephras are labeled according to Braitseva et al. (1997, 1998) and Ponomareva et al. (2013a, 2015). Shiveluch tephras are labeled SH followed with the number of the unit according to the proximal nomenclature (Ponomareva et al., 2015); old labels for several regional marker tephras are provided in brackets and follow Braitseva et al. (1997). Ages are given as 2 sigma intervals and weighted mean values according to our age model.
Ponomareva et al. "A full Holocene tephrochronology for the Kamchatsky Peninsula region: applications from Kamchatka to North America".

Electronic Supplement Figure, using data from Supplementary Table A.4, which shows data on reference microprobe materials analyzed, except for three major standards, as unknowns in the course of this study.

We obtained a total of 2778 individual glass analyses in the study area (Electronic supplement Table A.2) and 318 analyses on reference proximal tephras. For identification and correlation of marker tephras we compared our dataset to the reference analyses and to those published by Bourgeois et al. (2006), Kyle et al. (2011), Ponomareva et al. (2013a, 2015), and Plunkett et al. (2015), with the help of bi-plots in some cases supplemented with statistical analysis. Statistical comparison of Shiveluch tephras to their proximal counterparts was performed with the help of a recently published interactive table (Ponomareva et al., 2015). For statistical comparison we used a similarity coefficient (SC, Borchardt et al., 1972) and *t*-test (Microsoft Excel). In the case of heterogeneous tephras (mostly from Shiveluch and Kliuchevskoi volcanoes) bi-plots appeared to be more useful than statistical analysis.

4. Results

4.1. Stratigraphy and ages

Detailed tephra stratigraphy for six key sections is presented in Fig. 4a–d. Characteristics of tephra layers from key sites can be found in Electronic Supplement Table A.1. Tephras are represented mostly by light-colored (pale yellow, light-gray), very fine to medium ash. Several layers are coarse ash of specific "salt-and-pepper"

appearance caused by the presence of a large amount of plagioclase and dark minerals (amphibole, iron oxides, and pyroxene) specific to Shiveluch tephra (Braitseva et al., 1997). In addition, all sections contain up to seven layers of dark-gray or black, cindery ash. The characteristic appearance of tephra layers and their stratigraphic consistency help us correlate layers among closely spaced sections without additional geochemical data.

Four regional marker tephra layers run through the whole study area and can be easily identified in the field based on their position in the section along with color, grain size and grading. These are from top to bottom: (1) coarse salt-and-pepper SH1964 ash from the 1964 Shiveluch eruption (Gorshkov and Dubik, 1970); (2) pale yellow (with grayish top) fine 1.7 ka KS_1 ash from Ksudach caldera-forming eruption (Braitseva et al., 1996, 1997; Pevzner et al., 1998; Pinegina et al., 2013b); (3) normally-graded (from medium to fine-grained) yellow 4.7 ka SHdv ash from Shiveluch (Bourgeois et al., 2006), and (4) 3–8 cm thick, coarse black cindery 10.2 ka PL2 tephra positioned close to the bottom of the Holocene tephra sequence (Ponomareva et al., 2013a). These tephra layers form the major stratigraphic framework for the Ust-Kamchatsk area and permit the division of the Holocene tephra sequence into several intervals. Further stratigraphic constraints are provided by compositionally unique tephras SH#28 (SHsp), IAv12 (AV_4), KS_2 and PL1.

4.2. Geochemical data

All glass data for the key sections are shown in Fig. 5a and b. All glasses fall between 54 and 81% SiO_2, and based on their K_2O contents belong to four major series: (1) andesite to rhyolite low-K trend; (2) basaltic andesite to dacite medium-K trend; (3) dominantly rhyolite medium-K field with some scatter to high-K Si-rich rhyolites; (4) basaltic andesite to andesite high-K trend. Two medium-K fields are separated by a gap between 66 and 69% SiO_2. The observed array of glass compositions suggests that our study area has experienced tephra falls from different volcanic zones. Comparison of our new dataset to earlier published data for the study area shows that most of the analyses in Bourgeois et al. (2006) suffer dramatic Na_2O loss so have only limited use for correlations (Fig. 5c). To account for Na loss Kyle et al. (2011) used averaged Na_2O values; their data are more consistent and will be used for comparisons.

(1) The low-K trend extends from 63 to 77% SiO_2 and is well defined on the K_2O-SiO_2 diagram (Fig. 5a). On the CaO-SiO_2 diagram, however, the trend splits into two separate fields, with the most silicic glasses having distinctly higher CaO contents (Fig. 5d). This pattern suggests that the study area received ash falls from different low-K sources. Low-K compositions are characteristic of volcanic rocks erupted in the frontal, coast-proximal part of the Kamchatka volcanic belt (Volynets, 1994). Regional marker tephras from this volcanic zone are associated with Ksudach and Avachinsky volcanoes (Fig. 1a; Braitseva et al., 1997; Kyle et al., 2011). Comparison of our data to reference compositions of KS_1, KS_2 and IAv12 (AV_4) (Kyle et al., 2011; Electronic Supplement Table A.2) shows that all three tephras are present in our study area: KS_1 appears in all the key sections, KS_2 in Duma and Krutoberegovo (the only sections with deposits older than 5 ka), and IAv12 – in Duma and Cherny Yar (Fig. 4a,c and 6; Table 2). KS_1 glass compositions form a short trend between 71.5 and 75.2% SiO_2, while KS_2 glasses form a longer trend in the dacite-rhyolitic field. AV_4 glasses are more Si- and Ca-rich than Ksudach ones (Fig. 5c).

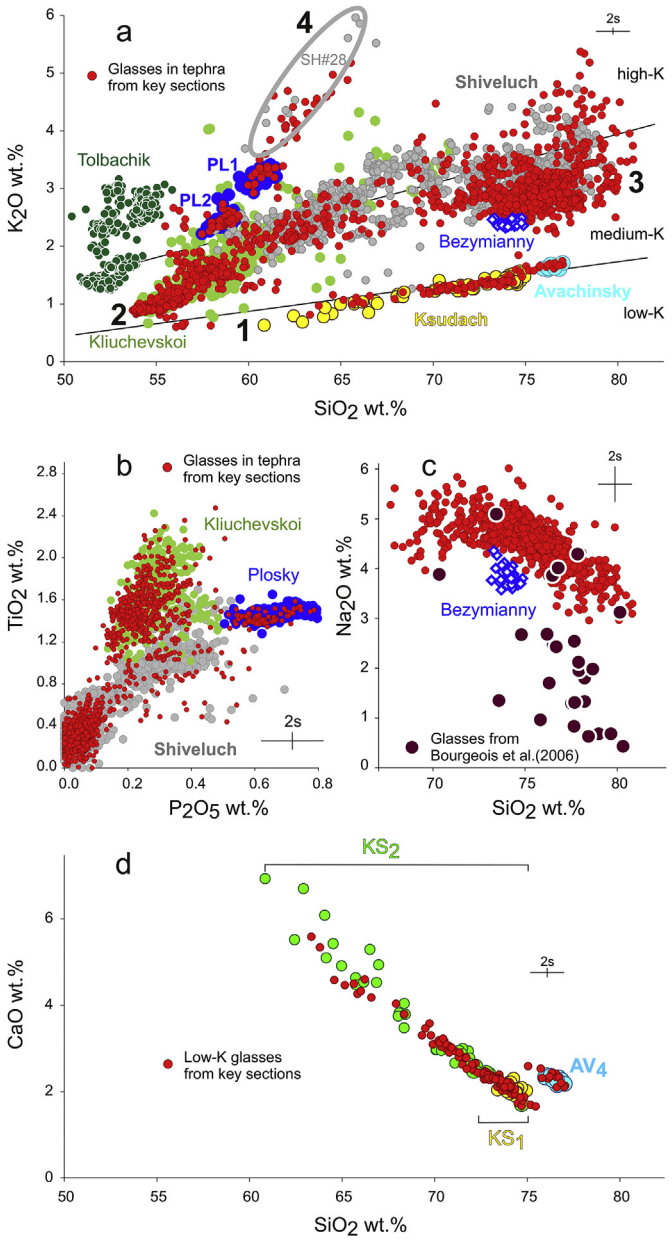

Fig. 5. Chemical composition of volcanic glasses from tephra from key study sections. **a.** Comparison of study-area glasses (red circles) to reference data for source volcanoes (symbols and labels for each volcano shown in matching colors). Numbers indicate four major compositional trends defined by their K_2O contents (see explanations in the text). The fields of low-, medium-, and high-K rocks are according to Gill (1981). Gray outline embraces data points for SH#28 (SHsp) tephra. Reference data here and in following graphs: *Ksudach* – Kyle et al. (2011); *Plosky* – Ponomareva et al. (2013a); *Shiveluch* – Ponomareva et al. (2015); *Kliuchevskoi* – Ponomareva et al. (2013a); Portnyagin and Ponomareva, unpublished data; *Avachinsky, Bezymianny*, and *Tolbachik monogenetic lava field* – Electronic Supplement Table A.2. **b.** TiO_2-P_2O_5 diagram permits differentiation between basaltic andesite – andesite glasses from the study area. **c.** Comparison of new glass data for Kamchatsky Peninsula to Bezymianny glasses (Electronic Supplement Table A.2) and data from Bourgeois et al. (2006). **d.** Comparison of low-K glasses from the Kamchatsky Peninsula key sections to reference Ksudach and Avachinsky (IAv12 or AV_4) glasses (Kyle et al., 2011; Electronic Supplement Table A.2). Brackets show SiO_2 range for KS_2 and KS_1 glasses. Analytical uncertainty of single points is expressed as 2 standard deviation (2s, 95% probability) and estimated using long-term reproducibility data on reference glasses for typical compositional range shown on each diagram on this and following figures. Interactive electronic spreadsheet to estimate 2s uncertainty and its dependence on glass composition is provided in Electronic Supplement Table A.4. (For interpretation of the references to colour in this figure legend, the reader is referred to the web version of this article.)

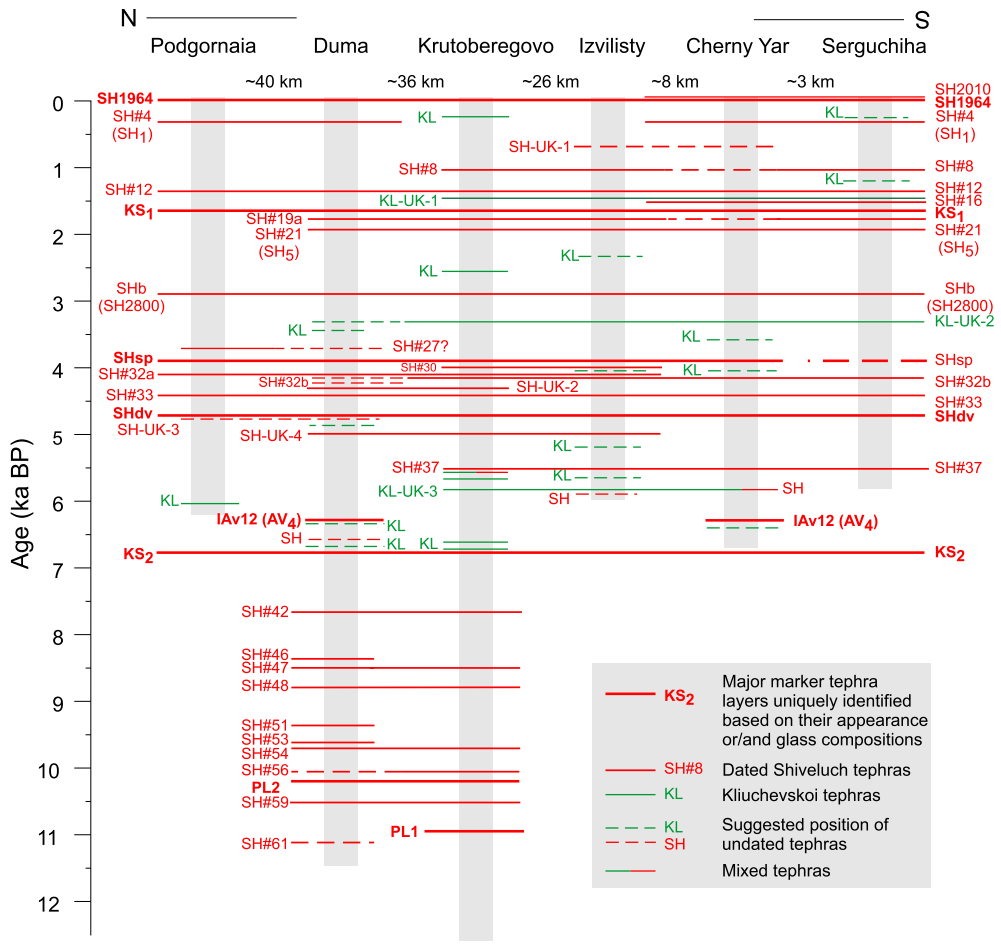

Fig. 6. Schematic summary tephra sequence for the study area. Major marker tephra layers uniquely identified based on their appearance and/or glass compositions are shown in bold lines and codes. Other tephras are shown in thin red (Shiveluch) and green (Kliuchevskoi) lines – solid for dated tephras and dashed where age or correlation is not definitive. (For interpretation of the references to colour in this figure legend, the reader is referred to the web version of this article.)

(2) The medium-K basaltic – andesite-dacite trend likely encompasses both basaltic andesite-andesite glasses from Kliuchevskoi and andesite-dacite glasses from Shiveluch (Fig. 5a and b). Four Kliuchevskoi tephras were tentatively reported in Cherny Yar peat by Pevzner et al. (1998) based on their cindery appearance. Mafic medium-K Shiveluch tephras have never been reported beyond Shiveluch slopes. Glasses from the Tolbachik monogenetic cinder cones form a separate field on the bi-plots, which does not overlap with that from the study area (Fig. 5a). This separation suggests that Tolbachik tephras were not deposited as visible layers over the Kamchatsky Peninsula area.

(3) The medium-K to high-K dominantly rhyolite field likely includes only Shiveluch glasses (Fig. 5a). Another potential source of silicic tephra from the Kliuchevskoi group is Bezymianny volcano; however, Bezymianny glasses contain less K and Na than the rhyolitic glasses from the study area (Fig. 5a, c).

(4) The high-K andesite-dacite trend comprises glasses from the Plosky PL1 and PL2 tephras (Ponomareva et al., 2013a) as well as from Shiveluch basaltic tephra SH#28 (SHsp) (Volynets et al., 1997; Ponomareva et al., 2015). Presence of PL1 and PL2 was previously reported from the Krutoberegovo site (Ponomareva et al., 2013a); in addition, PL2 tephra is present in the Duma section (Fig. 4d). SH#28 tephra was previously identified in Cherny Yar by Pevzner et al. (1998) and also in Podgornaia based on a few glass analyses by Bourgeois et al. (2006). Based on the overall dispersal of this tephra shown in Volynets et al. (1997) SH#28 should be present in the entire study area. Comparison of our data to reference glass compositions (Fig. 5a) confirms presence of SH#28 in Duma, Krutoberegovo, Izvilisty and Cherny Yar.

In summary, as a result of initial screening of our EMP data we have confirmed presence of six regional marker tephras: 1.7 ka KS_1, 3.9 ka SH#28 (SHsp), 6.3 ka IAv12 (AV_4), 6.8 ka KS_2, 10.2 ka PL2, and 11 ka PL1 in our sections. We will use these tephras as primary stratigraphic markers to divide the tephra sequence into several intervals for practical comparison (Fig. 4a–d and 6). Our data also confirm the presence of numerous Shiveluch and Kliuchevskoi tephras. Below we present details on Shiveluch tephras that can serve as reliable markers for the study area and examine the usefulness of cindery Kliuchevskoi tephras as markers.

4.3. Identification of tephra layers between major marker tephras

4.3.1. Top to KS_1 (0–1.7 ka)

The tephra sequence from the top (present) down to KS_1 contains two historical (SH2010 and SH1964) and four to six prehistorical tephra layers (Fig. 4a). The two historical tephras, both from Shiveluch, serve as type products for a plinian (SH1964) and a dome-related (SH2010) eruption. SH2010 tephra (~0.1 km^3) is

related to a currently growing Shiveluch lava dome (Zharinov and Demyanchuk, 2013). SH2010 glasses contain distinctly more SiO_2 (77.8–80.2%) compared to SH1964 ones (74.4–75.8%) and are depleted in Cl, which suggests their origin from a shallow, evolved and degassed magma chamber (Fig. 7a,b; Ponomareva et al., 2012).

The SH1964 eruption produced tephra fall and pyroclastic density current deposits with a total volume of 0.6–0.8 km^3 (Gorshkov and Dubik, 1970). Its glass compositions from two sites (Duma and Krutoberegovo) are similar to each other (SC = 0.913) though average CaO, Na_2O and K_2O are different with 99% probability on the basis of *t*-test (Fig. 7a, b). Detailed inspection shows that Duma glass composition is most close to that from the proximal SH1964 fall deposits (SC = 0.940), while Krutoberegovo glasses have compositions more similar to that of the SH1964 ignimbrite (SC = 0.946). Glasses from the fall deposits have slightly (~7 rel.%) but systematically lower K_2O contents compared to those

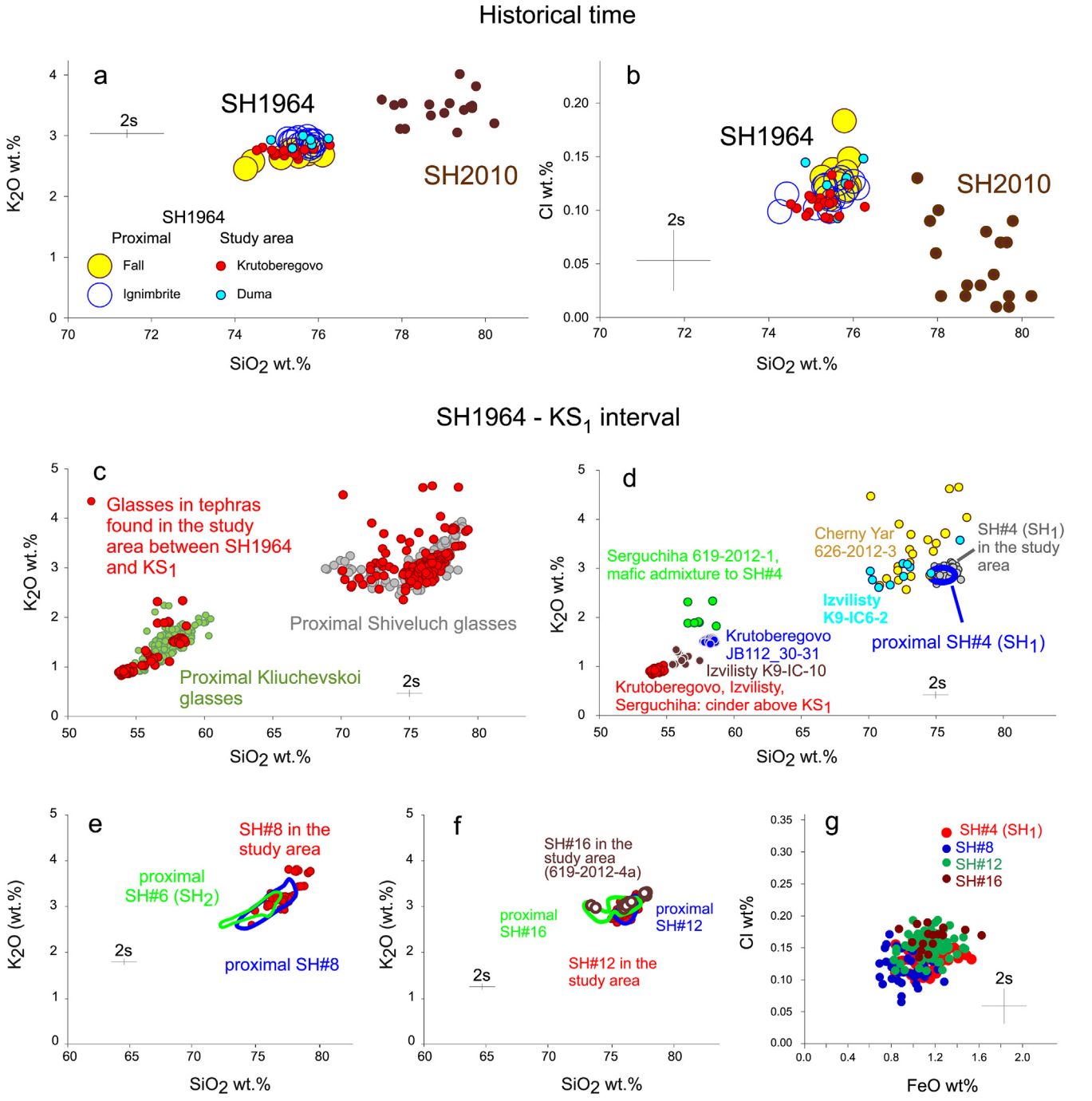

Fig. 7. Composition of glasses from tephra layers deposited in the study area during the last ~1700 yrs: **a** and **b** – historical Shiveluch tephras derived from large plinian (SH1964) and moderate dome-related (SH2010) eruptions; **c** – comparison of study-area glasses to reference compositions from Kliuchevskoi and Shiveluch volcanoes from the same stratigraphic interval; **d** – **g** – examples of geochemical diagrams used for tephra correlations based on glass major element compositions: **d** – comparison of Kliuchevskoi and selected Shiveluch glasses between different key sections; gray circles combine SH#4 glasses from four key sections; **e** – comparison of glasses in SH#6 and SH#8 tephras; **f** – comparison of glasses in SH#12 and SH#16 tephras; **g** – comparison of Cl and FeO contents in glasses of four major Shiveluch tephras between SH1964 and KS_1. Symbols and labels for each tephra are shown in matching colors; in diagrams **d-f** color outlines embrace compositions of proximal tephras under comparison.

from the ignimbrite. Such variability indicates presence of both fall and co-ignimbrite ash within the same distal tephra layer and may be expected in some other layers as well.

Most tephra layers between SH1964 and KS_1 are composed of light-colored, fine to coarse ash. In addition, the sections contain several ≤1 cm thick layers of black, fine cindery ash (Fig. 4a; Electronic Supplement Table A.1). Glasses from this interval clearly fall into the Kliuchevskoi and Shiveluch fields (Fig. 7c). Only one Kliuchevskoi tephra – the layer immediately above KS_1 with an age of ~1.35 ka – can be correlated among several sites (Fig. 7d). Its low-Si composition – the lowest in the Kliuchevskoi field – helps to differentiate it from the other cinders in this stratigraphic interval and fits into the previously established wave-like compositional variability of Kliuchevskoi proximal glasses with changes from low-Si (~55% SiO_2) to high-Si (65–70% SiO_2) glasses over ~1.5 ka (Portnyagin et al., 2009; Ponomareva et al., 2012). As this newly characterized tephra can work as a marker for the study area we labeled it KL-UK-1 (Fig. 6).

Most Shiveluch glasses are very similar in composition and form a compact field between 74.6 and 78% SiO_2 (Fig. 7c). Only one tephra with heterogeneous glasses clearly stands apart and possibly correlates between the Izvilisty and Cherny Yar sections (SH-UK-1, Figs. 6 and 7d). Although glasses of similar compositions are known in the proximal dataset for this interval (Fig. 7c), there are no exact matches to the described tephra, so it was probably derived from a heretofore-unidentified dome-related eruption.

Based on earlier descriptions of tephras at the Cherny Yar and Podgornaia sites (Pevzner et al., 1998; Bourgeois et al., 2006), the expected Shiveluch tephras in this interval would be SH#4 (SH_1), SH#6 (SH_2), and SH#12 (SH1450). At both sites the upper tephra is a very fine to fine ash and the two others are medium to coarse ash. Geochemical correlations of the glasses (Fig. 7d–f) along with the tephra stratigraphy (Fig. 4a) confirm presence of SH#4 and SH#12 tephras in the area, whereas the coarse tephra between them, supposedly SH_2 (SH#6), better matches SH#8 (Figs. 4a and 7e; Table 2). An additional Shiveluch tephra is present in Cherny Yar and Serguchiha sites, below the others and closer to KS_1. The closest match in the proximal database is SH#16 (Figs. 4a and 7f). Homogeneous glasses of this interval have only slight variations in Cl and FeO contents (Fig. 7g). SH#4 and SH#8 tephras are related to ignimbrite-forming eruptions (Ponomareva et al., 2015) and have slightly lower Cl contents possibly explained by the presence of a more degassed co-ignimbrite ash.

4.3.2. KS_1 to SH#28 (SHsp) (1.7–3.9 ka)

Tephras in this interval plot into the Kliuchevskoi and Shiveluch fields, which can be further discriminated based on Na_2O content, which is lower for Kliuchevskoi (Fig. 8a). Two major Shiveluch markers – SH#21 (SH_5) and SHb (SH2800) – run through most of the sections (Fig. 4b, Table 2). SH#21 glasses have higher SiO_2 and lower Cl compared to SHb (Fig. 8d). In Podgornaia only SHb is present; the distribution of SHb coincides with its preliminary mapping based on direct tracing (Pevzner et al., 1998; Kyle et al., 2011). SH#21, however, has not been previously mapped in the study area.

One to three thin Shiveluch tephra layers are present between KS_1 and SH#21 (Fig. 4b). A single tephra in Krutoberegovo and Izvilisty comprises two glass populations, mafic and silicic, matching SH#19a (Fig. 8c). In Duma, the upper and lower of three separate thin tephra layers include both of these glass populations (probably with some admixture of SH#19) indicating that SH#19a may be a product of different eruptions, closely spaced in time, rather than an eruption of bimodal composition. This set of tephras has never been reported beyond Shiveluch slopes and can serve as an additional marker.

Kliuchevskoi glass compositions in this interval change from 61 to 74% SiO_2 in the older tephra (sample 625-2012-3) to 54–55.5% SiO_2 in a younger tephra between SH#21 and SHb (sample JB112_197) (Fig. 8b). The most silicic glasses occur directly above the 3.8 ka SH#28 tephra, which is consistent with the proximal Kliuchevskoi record (Ponomareva et al., 2012). Only one Kliuchevskoi tephra (KL-UK-2) in this interval is present in several sections including Krutoberegovo, Izvilisty, Cherny Yar, Serguchiha, and likely Duma (Fig. 4b). Its glasses form a tight cluster in the bi-plots (Fig. 8b), which permits its designation as a marker tephra.

4.3.3. SH#28 (SHsp) to SH#34 (SHdv) (3.9–4.7 ka)

The lower boundary of this interval – SH#34 (SHdv) – is a normally graded, pale-yellow, very fine to fine ash easily traceable over the study area and identified in all studied sections (Figs. 4b and 6, Table 2). Its glasses form a trend in the rhyolitic field and match the silicic part of the proximal SH#34 trend (Fig. 8f). In different key sections tephra sequences between SH#28 and SH#34 comprise two to six Shiveluch tephras most of which are fine to coarse salt-and-pepper sands characterized by rhyolitic glasses (Figs. 4b and 8e; Electronic Supplement Table A.1). In addition, two dark-gray layers contain andesitic glasses typical for Kliuchevskoi tephra of this period (Portnyagin et al., 2011) and likely link Izvilisty and Cherny Yar sections (Figs. 4b and 8f).

Most of the rhyolitic glasses are very close in composition and form a tight cluster between 73.2 and 77% SiO_2 (Fig. 8e, g) which hampers their correlation and mapping over the study area. In previous studies, pumiceous tephras in this interval were labeled according their approximate ^{14}C ages either SH3700 or SH3800 (e.g., Bourgeois et al., 2006) although it was not clear which specific layer was present in any individual section. In the summary Shiveluch section, five tephras have been described in this interval and only four of them analyzed (Ponomareva et al., 2015).

Detailed comparisons of the geochemical data for rhyolitic glasses along with stratigraphic constraints suggest the following (tentative) correlations between the distal sections (this paper) and the Shiveluch proximal sequence (Figs. 4b and 6, Table 2). The best expressed marker that can be correlated to the proximal sequence is SH#33 at the bottom of this interval (Fig. 8f, Table 2). One more anchor point is the most silicic tephra in this interval which runs from Podgornaia to Duma, and probably also to Krutoberegovo and Izvilisty (Figs. 4b and 8). Its glass correlates to sample 96025-11 from the proximal Shiveluch sequence previously assigned to SH#32 together with the other, more mafic sample 00K19-1 (Ponomareva et al., 2015). Sample 00K19-1 in fact correlates to another, stratigraphically lower tephra in our study area (Fig. 4b). We suggest that the two proximal tephras previously combined into SH#32 in fact were produced by two different eruptions, and we have labeled them SH#32a and SH#32b (Fig. 4b). The thickness of SH#32a increases northward to up to 5 cm in Podgornaia so it was likely dispersed to the northeast (Figs. 1 and 4b) and corresponds to SH_{3700} in Bourgeois et al. (2006).

4.3.4. SHdv to KS_2 (4.7–6.8 ka)

This interval has fewer silicic tephras than the overlying ones, marking a period of about 2000 years with reduced volcanic impact on the study area (Figs. 4c and 6). The main regional marker within this interval is the 6.3 ka IAv12 (AV_4) tephra – a distal ash from Avachinsky volcano, present as a visible layer in the Duma and Cherny Yar sections (Figs. 4c and 9a).

The main Shiveluch marker in this interval is a layer of salt-and-pepper, coarse ash which runs through Duma, Krutoberegovo, Izvilisty, and likely Cherny Yar, and which stratigraphically and geochemically correlates to SH#37, with an age of ~5.5 ka (Figs. 4c and 9d, Table 2). One more link between Krutoberegovo, Duma and

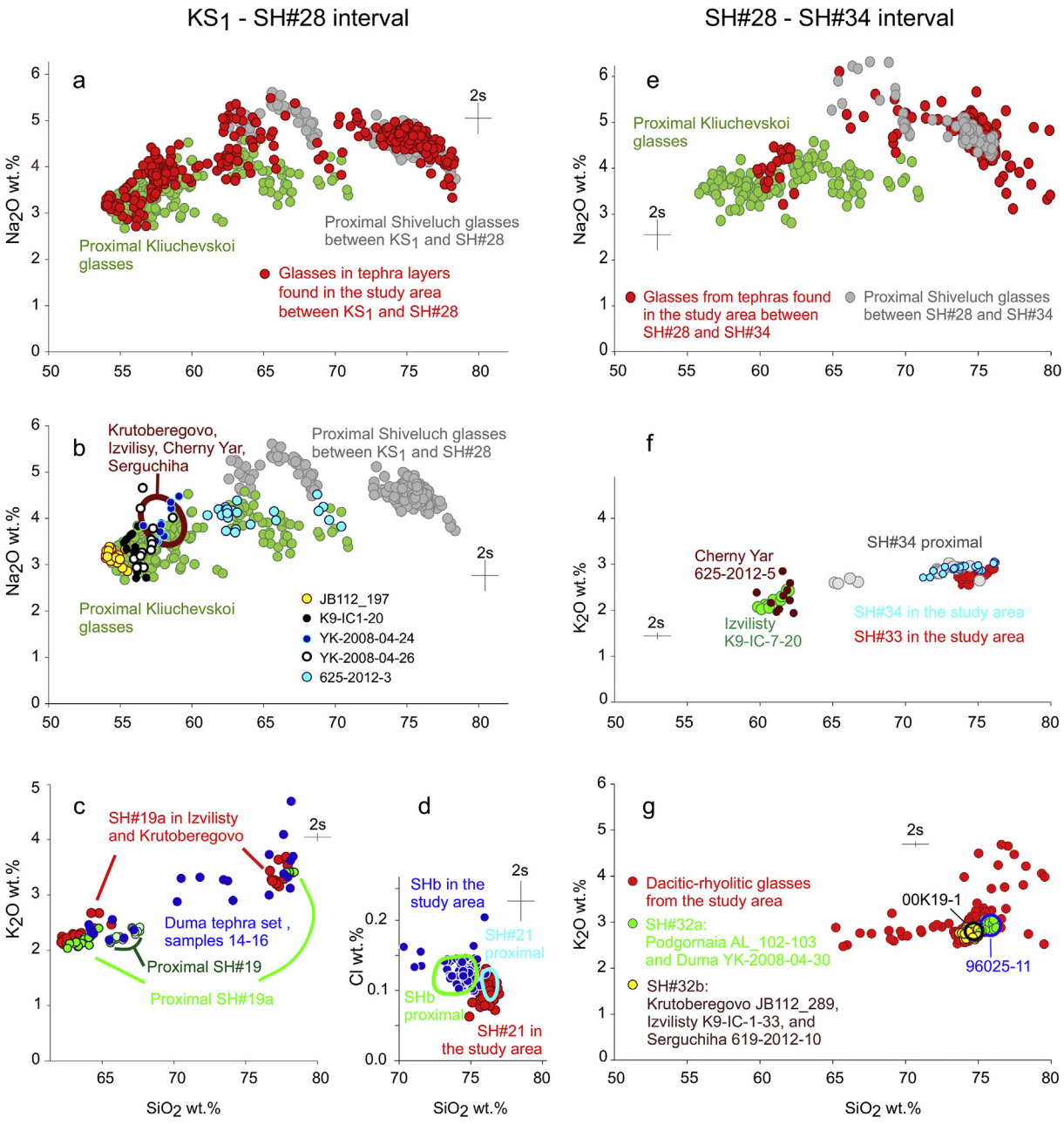

Fig. 8. Glass compositions in tephra layers within KS_1 – SH#28 (SHsp) and SH#28 – SH#34 (SHdv) intervals. Left column (KS_1 – SH#28 (SHsp) interval): **a** – comparison of study-area glass compositions to proximal Shiveluch and Kliuchevskoi glasses from the same stratigraphic interval; based on Na_2O contents, most dacitic glasses belong to Shiveluch; **b** – comparison of glasses from various cindery tephras in the study area to proximal Kliuchevskoi glasses from the same stratigraphic interval, composition of the single Kliuchevskoi tephra correlated between multiple sections is shown with the brown outline; **c** – multiple glass populations in SH#19 tephra likely comprising at least three Shiveluch tephras (see explanations in the text); **d** – comparison of glass compositions in SH#21 and SHb tephras, color outlines show proximal glass compositions of the tephras under comparison. Right column (SH#28 – SH#34 (SHdv) interval): **e** – comparison of glass compositions found in tephras in the study area relative to proximal Shiveluch and Kliuchevskoi glasses from the same stratigraphic interval; based on Na_2O contents, most dacitic glasses belong to Shiveluch; **f** – comparison of glasses from SH#34 (SHdv) tephra from the study area to proximal ones; SH#33 and SH#34 glasses from the study area show difference in K_2O in closely spaced in time Shiveluch tephras; and comparison of dacitic glasses from the Kliuchevskoi tephra linking Cherny Yar and Izvilisty sections; **g** – differentiation between the two tephras earlier erroneously assigned to the same proximal Shiveluch unit SH#32 (Ponomareva et al., 2015): this unit likely represents two tephras (labeled SH#32a and SH#32b in this study) with distinctive glass compositions. Color outlines embrace glasses from the two samples (00K19-1 and 96025-11) earlier included into the same unit SH#32. (For interpretation of the references to colour in this figure legend, the reader is referred to the web version of this article.)

likely Izvilisty is provided by a thin SH-UK-4 tephra at the top of the interval (Figs. 4c, 6 and 9d). Tephra compositionally similar to this thin tephra has not been identified on the volcano slopes (Fig. 9a; Ponomareva et al., 2015) so is a new addition to Shiveluch eruptive history. This interval includes a few thin Shiveluch tephras which we cannot correlate between the sections. Most Shiveluch tephras within this interval are characterized by high SiO_2 and K_2O, and low Cl contents, which suggest their origin from dome-related activity likely fed from a shallow, evolved and degassed magma chamber (Fig. 9 a–c).

Only one cindery Kliuchevskoi tephra layer in this interval, labeled by us KL-UK-3, provides a reliable link between the

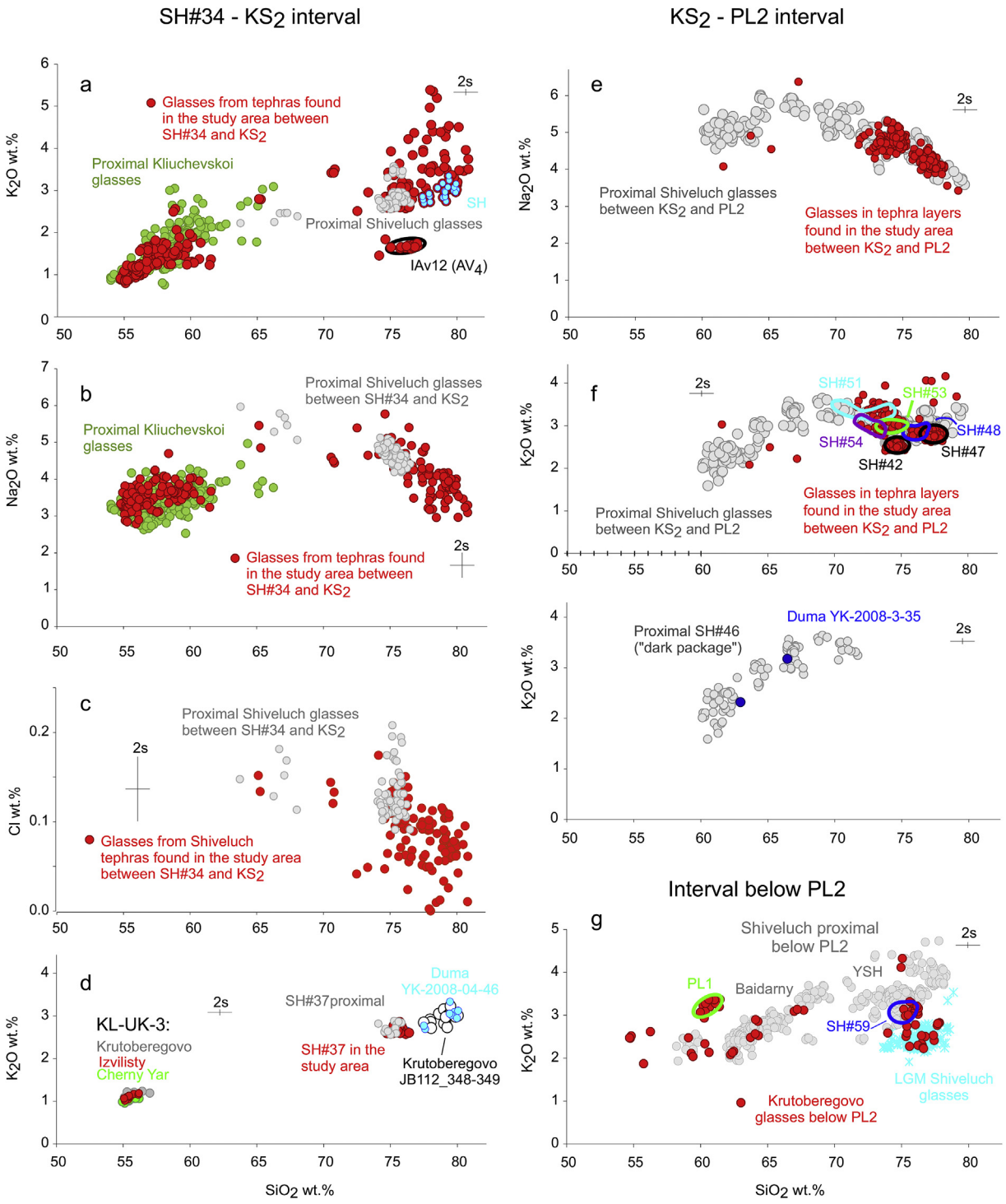

Fig. 9. Glass compositions in tephra layers within SH#34 (SHdv) – KS_2, KS_2 – PL2, and below PL2 intervals. Left column (SH#34 (SHdv) – KS_2): **a, b** – comparison of glass compositions found in tephras in the study area relative to proximal Shiveluch and Kliuchevskoi glasses from the same stratigraphic interval. Reference data for IAv12 (AV_4) tephra is shown with black outline. Blue circles show a newly identified Shiveluch tephra (SH, Fig. 4c) not described in the proximal sequence; **c** – Cl contents in most Shiveluch glasses in the study area is lower than that in glasses from pumices in proximal dataset, and likely indicates their origin from shallow degassed magma chamber feeding the lava dome; **d** – comparison of Kliuchevskoi glasses in the same tephra sampled in different outcrops, and of two Shiveluch tephras: SH#37 in the study area and proximal sequence, and newly identified SH tephra sampled in Krutoberegovo and Duma. Right column, **e** – **g** (KS_2 – PL2 interval): **e** – only high-Si glasses from Shiveluch tephras are found in this interval; **f** – attempts to differentiate glasses from individual Shiveluch tephras, color outlines embrace glass compositions from tephras identified in the proximal Shiveluch sequence; **g** – glasses from SH#46 ("dark package") compared to glasses found in the study area. Right column, lower diagram **h** (below PL2): identification of PL1, SH#59, Baidarny, and Shiveluch Late Glacial Maximum (LGM) tephras. Shiveluch activity in the LGM – late glacial time was presented consecutively by tephras with relatively low-K glasses from Old Shiveluch, Baidarny cinders, and early tephras from Young Shiveluch eruptive center (YSH) (Ponomareva et al., 2015). Glassed from all these tephras were found in Krutoberegovo sequence. Blue outline shows glass compositions from the proximal SH#59 tephra. (For interpretation of the references to colour in this figure legend, the reader is referred to the web version of this article.)

Krutoberegovo, Izvilisty and Cherny Yar sequences (Figs. 4c and 9d). Others differ from each other and likely represent different Kliuchevskoi eruptions (Fig. 9a–b).

4.3.5. KS_2 to PL2 (6.8–10.2 ka)

Tephra sequences below the KS_2 marker were found in only two sites: Duma (three sections) and Krutoberegovo (Fig. 4d). All sections contain six well expressed layers of light-colored coarse ash and one of dark-gray fine ash. At Krutoberegovo, the stratigraphy is complicated because the middle part of this interval contains abundant wood remains buried in bioturbated peat. As a result, tephra layers are partly disturbed, and pumice grains are scattered throughout (Fig. 4d). Thus we take only the Duma tephra sequence as the basis for the regional tephra stratigraphy in this interval.

Most glasses in this interval fall into a rhyolitic field compatible with proximal Shiveluch compositions (Fig. 9e). The upper pumice layer in Duma and Krutoberegovo correlates to SH#42 (Fig. 9f, Table 2). Glasses from this tephra have characteristically low K_2O contents unique for Shiveluch tephra in this interval. At Krutoberegovo, the same pumice is scattered throughout the peat from 556.6 cm down to ~625 cm interlayered with scattered pumice from SH#47 (Figs. 4d and 9f). The dark-gray tephra between SH#42 and SH#47 in the Duma section is likely mafic tephra SH#46. This tephra is highly crystallized so we had to sort out its analyses contaminated by microlites entrapment, but its appearance and stratigraphic interval suggest its identification as SH#46 and correlation to JB112_614-616 layer (Fig. 9g). Below SH #47, the Duma section contains tephra layers correlating to (from top to bottom) SH#48, #51, #53 and #54 (Figs. 4d, 6 and 9f; Table 2). Tephras SH#48 and #54 are present as well in Krutoberegovo, which also contains SH#56 lying directly above PL2 (Figs. 4d and 9f).

4.3.6. Below PL2 (bottom of the tephra sequence, 10.2–14.5 ka)

The upper tephra layer in this interval in both Krutoberegovo and Duma is likely SH#59 (Figs. 4d and 9h, Table 2), and the lower layer in Duma is likely SH#61. No visible tephra layers are present in Krutoberegovo below SH#59, but the three lowermost samples contain scattered volcanic glass. PL1 glasses from Plosky volcano are present in Krutoberegovo at 682–683 cm (Fig. 9h; Ponomareva et al., 2013a). Examination of glass shards from the two lowermost samples (Fig. 4d) brought surprising results because both samples contain low-Si (andesite to dacite) and high-Si (rhyolite) glasses (Fig. 9h). Most of the low-Si glasses perfectly fit into the Late Glacial Baidarny trend from Shiveluch volcano (Ponomareva et al., 2015). Baidarny-type cinders are believed to have been erupted since at least 16 ka, calculated based on average accumulation rate of the deposits (Pevzner et al., 2013). High-Si glasses belong to a certain type of Shiveluch tephras found only in the LGM moraine or directly below post-LGM fluvial deposits (Fig. 9h; Electronic Supplement Table A.2). Such a correlation might indicate that sediments at the bottom of the Krutoberegovo section either formed during the LGM or are composed of reworked LGM deposits.

5. Discussion

5.1. Major tephra markers for the Kamchatsky Peninsula region

Fig. 6 and Table 2 present major tephra markers for dating and correlating Holocene deposits and landforms in the study area. Glasses from twenty-nine major tephra markers and twenty nine other tephras have been analyzed in order to provide a reference database for identification in the study area and beyond (Fig. 5a, b). Tephra layers deposited in the study area are mainly from Shiveluch and Kliuchevskoi volcanoes. Two of the oldest tephras are related to the Plosky volcanic massif, two primary markers – to Ksudach caldera-forming eruptions, and one primary marker – to Avachinsky volcano. No Bezymianny or Tolbachik tephras have been identified in this area.

The main tephrochronological framework is formed by eight widespread tephra layers uniquely identified based on their appearance and/or glass composition. These are (from top to bottom): SH1964, 1.7 ka KS_1, 3.9 ka SH#28, SH#34, 6.3 ka IAv12, 6.8 ka KS_2, 10.2 ka PL2, and 11 ka PL1 tephras (Table 2). Glasses from the regional Ksudach (KS_1 and KS_2) and Avachinsky (IAv12) tephras are characterized by low-K composition; Avachinsky glasses have higher SiO_2 and CaO contents compared to Ksudach (Fig. 5d). Shiveluch SH#28 (SHsp) and Plosky PL1 and PL2 glasses form a distinct high-K trend in the andesitic field and differ from andesitic Kliuchevskoi glasses (Fig. 5a,b). These major tephras were used to split the Holocene sequence into several intervals to facilitate correlations of the interbedded tephras.

Of twenty-two Kliuchevskoi tephra layers analyzed in the study area only three can be correlated among two or more key sections (Fig. 6). Glass compositions of Kliuchevskoi tephra in the study area change through time from low-Si andesite (~5.7 ka) to hi-Si andesite (~4 ka) and then back to basaltic andesite (~1.4 ka) following a wave-like pattern established for the proximal deposits (Portnyagin et al., 2009). This variability permits differentiation between Kliuchevskoi tephras of different ages, adding to their usefulness.

Many Shiveluch tephras in this study are quite similar in appearance and glass composition, which is common at frequently erupting andesitic volcanoes (e.g., Donoghue et al., 2007). At the same time, their glasses also have variations in SiO_2 content through time (Ponomareva et al., 2015), which in many cases allows for differentiation (e.g., Fig. 9f). The prominent Shiveluch tephras in the study area correlate to known proximal tephra units (Fig. 6), with some amendments to earlier correlations. For example, a coarse salt-and-pepper tephra between SH#4 and SH#12 is likely SH#8 and not SH#6 (SH_2) as suggested earlier (Pevzner et al., 1998). Several Shiveluch tephras have unique glass compositions; for example, SHb and SH#34 (SHdv) glasses form trends in SiO_2 content while SH#42 glasses have the lowest K_2O contents among Shiveluch andesitic tephras (Figs. 7–9). In some tephra layers we found minor admixtures of compositionally different glasses (e.g., admixture of Kliuchevskoi glasses in the Shiveluch light-colored ash or of rhyolitic Shiveluch glasses in a cindery tephra). These admixtures suggest continuous activity from both volcanoes.

5.2. Identifying tephra layers in paleoseismological trenches and archaeological excavations

In undisturbed tephra-peat or tephra-soil sequences, stratigraphic position facilitates correlation of tephra layers, in addition to chemical fingerprinting. Clearly visible stratigraphy permits correlation not only of individual tephra layers but also of ordered sequences of tephra layers. On the contrary, in paleoseismological or archaeological excavations, individual layers or parts of tephra sequences may be out of stratigraphic context or be present as scattered patches (e.g., Figs. 3 and 11). Below we discuss several examples of tephra identification in such incomplete sequences. Selection of tephra layers for identification was based on the application for which the tephra layers were used.

Glass compositions for 48 “unknown” tephra samples from seven paleoseismological trenches, one peat section, and one lake core (Fig. 1b) are provided in Electronic Supplement Table A.2 and plotted in Fig. 10a against glasses from the key sections and reference glasses. “Unknown” glasses are split between the four series identified in section 4.2. In addition, differentiation between individual Shiveluch tephra layers was based on their stratigraphic

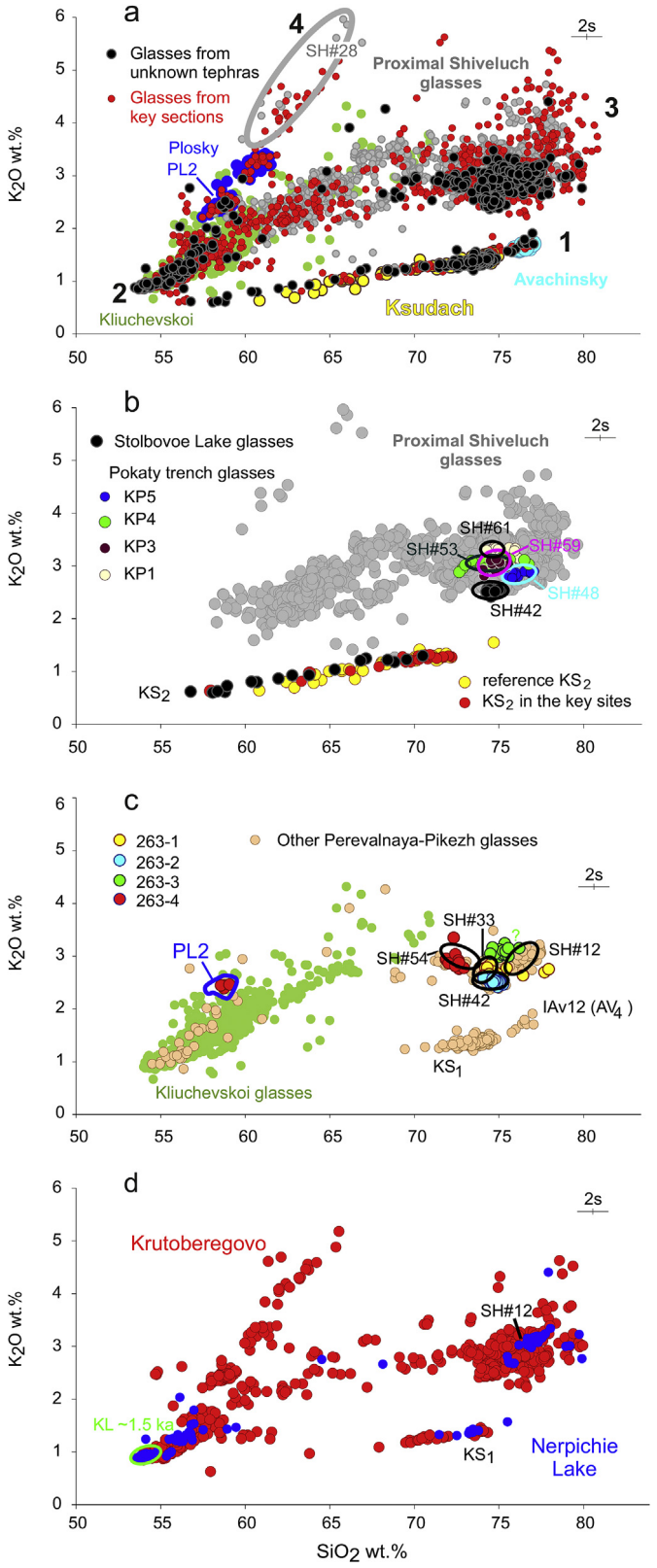

Fig. 10. Composition of glasses from tephras found in paleoseismological, paleoenvironmental and archaeological excavations and cores in the study area and treated as unknowns. **a** – comparison of unknown glasses to those from key study sections and from proximal Avachinsky, Kliuchevskoi, Ksudach and Shiveluch glasses, the latter group displayed in different colors; gray outline embraces data points for SH#28 (SHsp) tephra; **b** – identification of tephras in Stolbovoe Lake peat outcrop (Fig. 11a) and in Pokaty paleoseismological trench (Fig. 11b). Color outlines show glass compositions from different proximal tephra units; **c** – identification of tephras from the Perevalnaya – Pikezh area (e.g., Fig. 11c), outlines show glasses from proximal tephras as labeled; **d** – identification of major tephra layers in Nerpichie Lake core. Blue-green outline shows glass compositions from proximal Kliuchevskoi tephras erupted at ~1.5 ka (Ponomareva et al., 2012). (For interpretation of the references to colour in this figure legend, the reader is referred to the web version of this article.)

position between identified markers.

*5.2.1. **Paleoseismological** research in the study area includes dating of the deposits related to tectonic events such as tectonic uplift or subsidence, crustal faulting and tsunamis*

The **Stolbovoe Lake** bank escarpment (Figs. 1 and 11a) exhibits a ~3 m thick peat deposit overlying lagoon deposits. We used tephra layers to date the sharp transition between lagoon and peatbog conditions. The upper part of the tephra sequence therein is similar to that described for Podgornaia (Fig. 4a–c; Bourgeois et al., 2006): the 1.7 ka KS_1 tephra can be easily identified based on its appearance; and the thickness and grain size of the salt-and-pepper tephra below indicate it is likely SH#32a. Below SH#32a about ~1.6 m of peat follows containing a few less distinct tephra layers and lenses. We sampled the two lowermost tephra layers from the peat near the contact with the underlying lagoon deposits. Comparison of glass compositions from these samples to our data set permit identification of the upper layer as the 6.8 ka KS_2 and the lower tephra as the 7.7 ka SH#42 tephra (Fig. 10b) which is consistent with the stratigraphy and dates the onset of peat formation at 7.7–7.8 ka (Fig. 12). The **Pokaty paleoseismological trench** located close to Stolbovoe Lake and the Podgornaia key section (Fig. 1b) exhibits deformations related to collision of the Aleutian and Kamchatka arcs (Kozhurin and Pinegina, 2011). In the trench walls we identified four tephra layers below the well recognizable SH#34 (SHdv): SH#48, #53, #59 and #61 (Figs. 10b–12). While SH#42, #48, and #61 glasses differ from each other and from SH#53 and #59, glass compositions of the latter two tephras partly overlap so these tephras can be discriminated only when their stratigraphic position is clear. These tephra layers will help us to date early Holocene faulting events.

Selected tephra layers were identified in paleoseismological trenches in the **mountainous part of the Kamchatsky Peninsula** in order to date faulting events and calculate the rate of horizontal deformation caused by arc-arc collision. Soil-tephra sequences in this area are less thick and poorly preserved in comparison to those in the lowlands because of higher elevations and sparse vegetation (Fig. 1). In trench 263 (Fig. 1b) the tephra sequence overlies a river terrace cut by the strike-slip fault, which accommodates most of the onshore collision deformation (Kozhurin et al., 2014). Four better-preserved tephra layers (263–1 to 4 in Fig. 12; Electronic Supplement Table A.2) were sampled from the sequence in order to add stratigraphic constraints to their geochemical characteristics. The lowermost sample (sample 4) contains glasses from both 10.2 ka PL2 and 9.7 ka SH#54 tephras (Fig. 10c) and defines the minimal limit of the terrace age at ~10.2 ka. These data permit an estimate of the Holocene rate of horizontal deformation at 14–15 mm/year (Kozhurin et al., 2014). The two upper samples (1–2) are identified as SH#33 and SH#42 respectively, whereas the sample 263-3 between SH#42 and SH#54 does not match any known Shiveluch tephra (Ponomareva et al., 2015; Plunkett et al., 2015; this paper) and might represent a previously unrecorded eruption. Other trenches in the Pereval'naia-Pikezh area are located ~7 km south from the above-described trench and are ~3 km apart from each other. All four trenches contain SH#12 and KS_1; other identified tephras include SH#8, SH#33, IAv12 (AV_4), SH#42 and SH#54. (Figs. 10c–12). In some cases the same tephra layer is

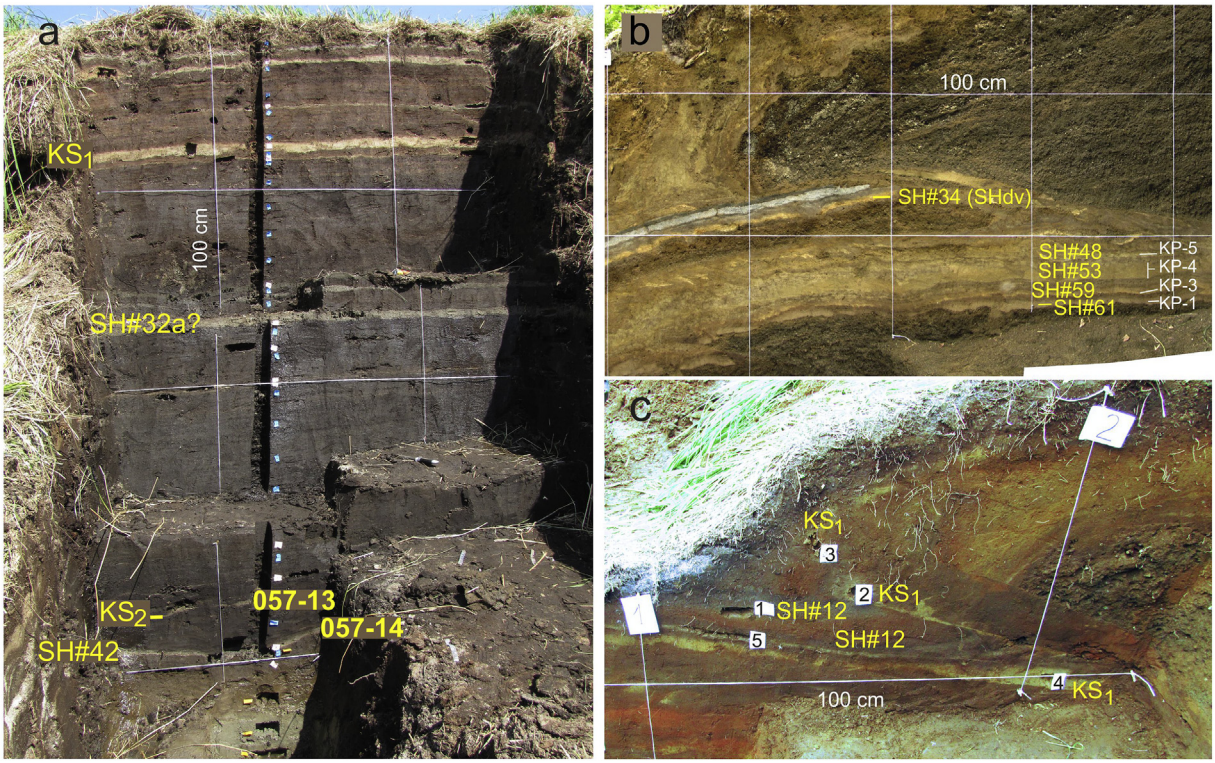

Fig. 11. Unknown tephras in a peat outcrop and paleoseismological trenches. Identified tephras (Fig. 10) are labeled in yellow. **a** – Stolbovoe Lake peat outcrop, 100-cm grid: two lower tephra layers were geochemically identified as KS_2 and SH#42, dating the onset of peat formation to ~7.8 ka; KS_1 was identified based on its unique appearance and SH#32a based on direct tracing to nearby Podgornaia site (Fig. 4b); **b** – tephra layers below SH#34 (SHdv) in Pokaty paleoseismological trench (detail), 100-cm grid; sample numbers are shown in white and match those in Fig. 10b; **c** – tephras in paleoseismological trench 526 in the Pereval'naia-Pikezh area, note patches and lenses of the same tephras disrupted by faulting and positioned on the top of original layers; white squares – locations of tephra, numbers correspond to those in Fig. 10c. (For interpretation of the references to colour in this figure legend, the reader is referred to the web version of this article.)

displaced by faulting, and patches or even layers of it appear several times at different levels on the trench wall (Fig. 11c).

At the **Izvilisty site**, the youngest faulting event horizon was more accurately stratigraphically positioned by the use of geochemical analysis of tephra. The disturbed horizon sandwiched between tephra layers preliminarily identified as SH#4 (SH_1) and SH#6 (SH_2), based on direct field tracing, was assigned an age of 300–800 a BP (Pinegina et al., 2012). Newly obtained geochemical characteristics, however, indicate that the upper of these tephra layers likely is SH-UK-1 tephra also present in Cherny Yar ~15 cm *below* SH#4 (SH_1), and the lower tephra corresponds to 1 ka SH#8 tephra (Figs. 3a, 4a and 7d). This correlation refines the stratigraphic position of the event horizon and suggests somewhat older age estimate of the faulting event (Fig. 12). Absence of SH#4 (SH_1) in all six Izvilisty excavations is hard to explain because it is well seen in both Duma and Cherny Yar sections (Fig. 1).

5.2.2. Archaeological excavations

Most sites in our study area have been occupied more than once, which adds to the complexities of tephra preservation (Pendea et al., 2016). However, detailed survey and mapping of the tephra layers in and especially directly outside house pits may permit tephrochronological dating of occupation layers (Pinegina et al., 2013a). While tephra layers will be removed during house excavation, debris left by people may be preserved between undisturbed tephra layers in sequences near the house pit. In Kultuk (Fig. 1b), for example, human-related debris (charcoal, pebbles, chopped angular rock fragments) was found between 1.7 ka KS_1 and 4.7 ka SH#34 (SHdv) tephra layers in a section beyond a house pit, whereas inside the house pit SH#34 had been removed and thus could not provide age control (Hulse et al., 2011).

Ancient people in the study area settled mostly on pre-Holocene lake and marine terraces or isolated hills, which now rise above the peatland but before about 6 ka were islands rising above a lagoon (Hulse et al., 2011; Pendea et al., 2016). One of the archaeological test pits on such a hill 160 m NNW of the main **Izvilisty** excavations exhibits a tephra sequence interrupted by three cultural layers (Fig. 1b; Hulse et al., 2011). Some tephra layers have been redeposited into the earlier existing depressions, and others occur as long broken lenses; however the general sequence of tephra layers can be inferred by examining all the walls of the pit (Fig. 3b). Analysis of selected tephra layers down from the 1.7 ka KS_1 tephra allowed us to identify SHb (SH2800), SH#33, SH#42, and SH#47 tephras (Figs. 3b and 12; Electronic Supplement Table A.2). The lower cultural layer is positioned between SH#33 and SH#47 and incorporates long horizontal lenses of SH#42, which form almost continuous layer. Although a single date on charcoal places the lower cultural layer around 4876-4588 cal BP (Hulse et al., 2011), the presence of almost continuous horizon of the 7.7 ka SH#42 tephra *above* the lower part of the cultural layer may indicate its older age. Additional in-depth analysis of tephra in archaeological context especially for the earlier Holocene, will provide more detailed time frameworks for human occupation of this region.

5.3. Identification of tephra layers in lake sediments

While peat can capture primary tephra-falls, lake sediments may in addition accumulate tephra washed into the lake from adjacent territories, which can make the lacustrine record more complex (e.g., Watson et al., 2016). Nerpichie Lake has an average

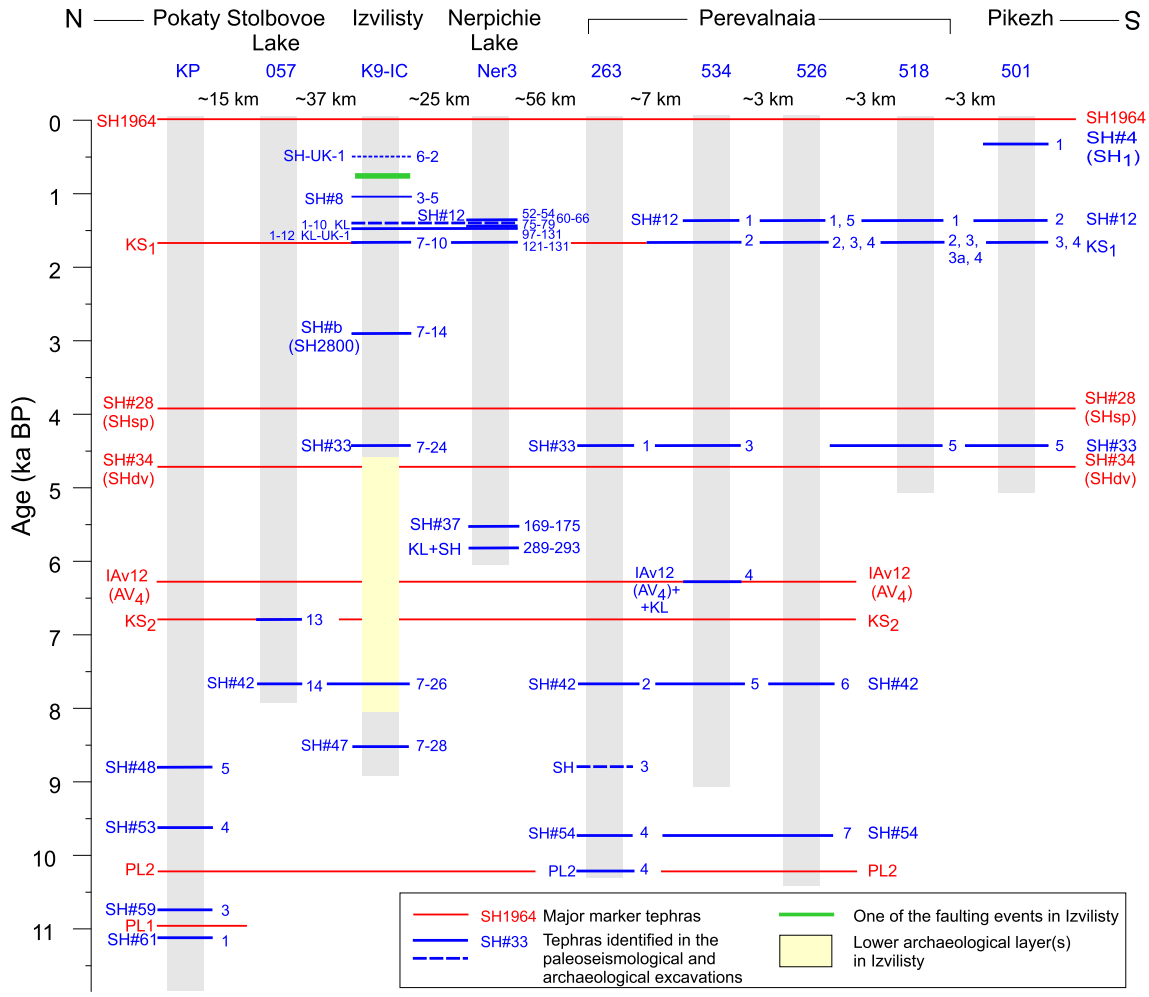

Fig. 12. Tephra layers geochemically identified (blue lines) in paleoseismological, paleoenvironmental and archaeological excavations and cores. Individual excavations or cores are shown as gray columns. Blue lines are dashed where age or correlation is not definitive. Red lines delineate (expected) major marker tephra layers identified based on appearance or/and glass composition. Samples IDs are in blue to the right of each column; a complete ID consists of the section ID (as at the top of each column) and sample ID. Distance (in km) shown between columns is distance between sections. (For interpretation of the references to colour in this figure legend, the reader is referred to the web version of this article.)

depth of 3.4 m and is connected to the ocean and to the Kamchatka River mouth through a narrow channel (Fig. 1). The lake is separated from the ocean by a 0.3–0.6 km-wide bar. The detailed history of the lake is not known but accumulation of its sediments was likely influenced by tectonic processes and changes in the sea level. A ~4 m long core taken in the lake (Cherepanova et al., 2013) recovered monotonous greenish-gray ooze. Unlike the peat sequences in the area, the lake sediments do not contain visible tephra layers except for SH1964.

Selected samples were wet sieved to obtain a >63 μm fraction, mounted in epoxy, and glasses were analyzed in profiles (every shard on the line). Examination of the data has proved that the glasses found in the upper part of the core provide a proper tephra succession down to the 1.7 ka KS_1 tephra matching the sequences in the nearby Krutoberegovo and Izvilisty peats (Figs. 10d and 12). The identification of the lower three samples is ambiguous because of an insufficient number of analyses. Glasses found below KS_1 probably correlate to SH#37; to a high-K Shiveluch tephra typical of the SH#34 – KS_2 interval; and to a ~5.8 ka cinder tephra from Kliuchevskoi also present at Krutoberegovo, Izvilisty and Cherny Yar (Fig. 6). Those correlations suggest that the onset of lake sediment accumulation roughly coincided with that of Izvilisty peat development (5.8 ka).

5.4. Contribution to volcanic histories

In Kamchatka, tephrochronological studies beyond the slopes of active volcanoes are limited (e.g., Pevzner et al., 1998, 2006) and only in some cases are supported by glass composition data (Dirksen et al., 2011; Kyle et al., 2011; Plunkett et al., 2015). The lack of distal data hampers compilations of tephra isopach maps and calculations of tephra volumes. The majority of the earlier correlations were based on direct tracing and radiocarbon dating (e.g., Braitseva et al., 1997; Pevzner et al., 2006, Pevzner, 2010) and still need evaluation with the help of geochemical data.

Our detailed studies in the Kamchatsky Peninsula area have allowed us to geochemically fingerprint tephras from five volcanic centers: the three more proximal Shiveluch, Kliuchevskoi and Plosky volcanoes, and two distant volcanoes, Avachinsky (~400 km) and Ksudach (~600 km) volcanoes (Fig. 1a). The presence of all these tephras on the central-eastern Kamchatka seaboard suggests they might also be present in sediment cores from the NW Pacific and the Bering Sea, as demonstrated, for example, by tephra PL2 from Plosky (Ponomareva et al., 2013a) and some early Holocene Shiveluch tephras (Ponomareva et al., 2015).

All three tephras from distant volcanoes are known in their proximal records (e.g., Braitseva et al., 1998; Volynets et al., 1999)

and have been previously mapped over a large part of Kamchatka (Braitseva et al., 1997, 1998; Kyle et al., 2011). At the same time, earlier published isopachs predicted presence in the study area of only one of these tephras, KS_1 (Fig. 1a). The known dispersal areas for KS_2 and IAv12 (AV_4) tephras can now be enlarged, shifting their eastern dispersal margins 55–80 km farther to the east (Fig. 1c).

Nine Shiveluch tephras present in the study area had not previously been reported on the volcano's slopes and thus are new additions to Shiveluch eruptive history (layers labeled SH-UK-1 to 4 and SH in Fig. 4a–c and 6, and SH#32 tephra split into two layers). The same underrepresentation of Shiveluch eruptions in the proximal record was reported by Plunkett et al. (2015) from their work north and southwest of the volcano. On the other hand, while many plinian eruptive clouds follow jet-stream patterns and are dispersed eastward, only 25 of 74 Holocene eruptions identified on Shiveluch slopes have deposited visible tephra layers in our study area. Our data suggest that none of the described distal sections contains a complete Shiveluch tephra sequence, which can be compiled only after distal tephras are identified in all directions from the volcano.

Recent ash falls from Kliuchevskoi have been reported in some villages on the peninsula, e.g., the 4th March 2015 eruption depositing 1 mm of ash on the snow cover in Ust'-Kamchatsk. Only two tephra layers in our record – SH1964 and SH2010 – can be linked to historical eruptions. None of the other ~50 historical eruptions left visible ash layers in the study area. No systematic study of pre-historical Kliuchevskoi tephras has been performed before so the timing and magnitudes of Kliuchevskoi's largest explosive eruptions are not known. Proximal record contains numerous cinder layers where individual eruptions have never been singled out (Portnyagin et al., 2009, 2011). Our record contains 22 Kliuchevskoi tephras, each 0.1–2 cm thick in the study region, and which all post-date the 6.8 ka KS_2 eruption. They therefore are presumably all related to construction of the modern cone (Braitseva et al., 1995). Three widely dispersed Kliuchevskoi tephras (KL-UK-1 to 3; ~1.5, 3.3, and 5.8 ka, respectively) correlate between several key sites (Fig. 6) so those are likely derived from relatively large eruptions. One more Kliuchevskoi tephra, directly above KS_2, although present only in Krutoberegovo, is 2 cm thick in this distant site so might also represent a large eruption, possibly corresponding to initiation of the modern cone (Braitseva et al., 1995). At 100–130 km distance from the volcano, a 2-cm-thick tephra could correspond to minimum deposit volumes of 0.20–0.25 km^3 (calculated according to Legros, 2000).

5.5. Recurrence rate of heavy tephra falls

The study area experiences minor ash falls on a regular basis, but most of those do not leave a visible tephra layer. Heavy tephra falls, however, may cause problems for human activities and livestock. In order to evaluate the recurrence rate of heavy ash falls (>0.5 cm thick), we are using the Krutoberegovo section as the longest and best preserved one in the area located close to local populations. In addition, it is the most distant key site from the dominant source volcanoes so it provides a minimum estimate of the tephra fall recurrence in the study region.

As summarized previously, the Krutoberegovo section contains 41 visible tephras deposited during the last ~11.5 ka including six redeposited layers and four mixed layers; the latter contain glass populations from Shiveluch and Kliuchevskoi or Shiveluch and Plosky (Fig. 4a–d; Electronic Supplement Table A.1). To provide a crude estimate of primary depositional thickness of disturbed tephras, we added thicknesses of redeposited layers to those of their parent layers. Four mixed layers (KL + SH or SH + PL) were considered as two layers each with half of the thickness of the mixed layer representing the primary thickness of each individual tephra. As a result, we obtained a sequence of 36 tephra falls with known sources and thicknesses (H) of tephra layers. This sequence was ranked (N) in order of decreasing thickness; thus for each layer, the corresponding value of N is the amount of *similar* or *thicker* tephra falls in the dataset. The average frequency through the time period considered here of events depositing a certain tephra thickness is calculated as n = N/11500 yr-1.

As a power-law frequency-size relationship has been shown by Gusev et al. (2003) for Holocene explosive eruptions in Kamchatka, we expect that the recurrence-versus-thickness data plotted on a logarithmic scale will form a linear trend. The obtained trends indeed are mostly linear (Fig. 13b), which suggests that the Krutoberegovo section agrees with the overall pattern observed in the suite of the Kamchatka explosive eruptions. The flattening of the trends for the thicknesses of <0.5 cm probably results from underrepresentation of thin tephra layers because of sampling and/or preservation bias. Eliminating data on thin layers, we obtain a more robust relationship between recurrence rate and tephra-fall thickness (Fig. 13b). Recurrence rate of heavy tephra falls (>0.5 cm) in Krutoberegovo is 0.0025 yr^{-1} (1 event in 400 years on average). Recurrence decreases with thickness, so recurrence rate of >1 cm tephra falls is 0.0012 yr^{-1} (1 event in 830 yrs on average). The same operation was conducted on subsets of Shiveluch (22 layers) and Kliuchevskoi (9 layers) tephras (Fig. 13a,b). Recurrence rate of Shiveluch heavy tephra falls is 0.0018 yr^{-1} (1 event in 550 years on average), and of Kliuchevskoi – 0.0004 yr^{-1} (1 event in 2500 years on average). Other volcanoes (Ksudach and Plosky) together deposited only four tephra layers in Krutoberegovo, which is not enough for analysis.

5.6. Links of tephra layers and environmental records far beyond the study area

Our dataset of glass compositions for the Kamchatsky Peninsula

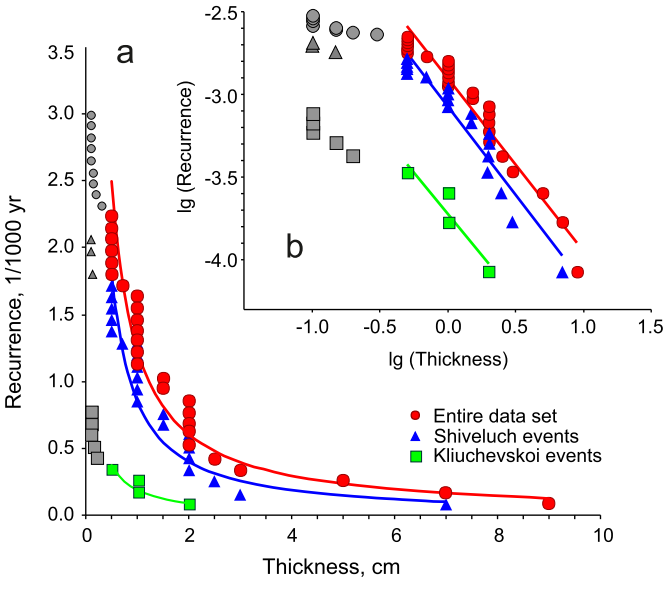

Fig. 13. Recurrence of heavy tephra falls (>0.5 cm thickness of a compacted tephra layer) for the Krutoberegovo site. Tephra-fall events per 1000 yr are plotted versus tephra thickness in both linear (a) and logarithmic (b) scales. Red dots show entire tephra dataset of the Krutoberegovo core, blue triangles show heavy Shiveluch tephra falls, green squares show heavy Kliuchevskoi tephra falls. Gray symbols show underestimated (i.e. having recurrence rate below trend line) events which are excluded from interpolation. (For interpretation of the references to colour in this figure legend, the reader is referred to the web version of this article.)

region serves as a reference for further tephra and cryptotephra research in a range of sites onshore and offshore east of Kamchatka. The primary marker tephras KS_1 and KS_2 directly link depositional sequences in the study area to archives located hundreds and thousands of kilometers away and thus provide an opportunity of synchronizing widely separated paleoenvironmental records. For example, the detailed Late Glacial-Holocene paleoenvironmental data obtained for Krutoberegovo site (Pendea et al., 2017) can be correlated to other Kamchatka paleoclimate records (containing KS_1 and KS_2 tephras) up to 340 km away in Stolbovaia, Uka, Esso and Ossora (Fig. 1a; Dirksen et al., 2013; Plunkett et al., 2015). Impressively recent identification of these tephras as far as ~8000 km away in eastern North America (S. Pyne O'Donnell, pers.comm; Mackay et al., 2016) provides direct intercontinental correlations of paleoenvironmental archives.

Two Shiveluch tephras identified in the study area (SH#56 and SH#59) have been found 560–580 km away in Bering Sea sediments, enabling direct comparison of terrestrial and marine paleoenvironmental data (Ponomareva et al., 2015). Although Shiveluch and Ksudach tephras have been mistakenly identified in the Aleutian Islands and in an ice core from Alaska (Ponomareva et al., 2015; Davies et al., 2016), Kamchatka tephras will definitely be identified in the Aleutians and farther away in future cryptotephra research. The sites in the Perevalnaya-Pikezh area are the easternmost tephra sites analyzed in Kamchatka (Fig. 1) which makes their tephra sequences especially interesting for (crypto)tephra research in the northwest Pacific marine cores, the Aleutian Islands, and North America.

6. Conclusions

This study is the first comprehensive tephrochronological-geochemical study of a major tephra repository of Kamchatka – in this case the Kamchatsky Peninsula region, a focus area important for paleoseismology, archaeology and paleoclimate. We have geochemically fingerprinted 58 Holocene tephras and used these data for identifying unknown tephras in archaeological sites, in lake and peat deposits, and in sequences disturbed by recent tectonic deformation. The main tephrochronological framework for the study area is formed by eight widespread tephra layers uniquely identified based on their appearance and/or glass compositions. These are three regional tephras (KS_1 and KS_2 from Ksudach and IAv12 from Avachinsky volcanoes), two tephras (PL2 and PL1) from the Plosky volcanic massif, and three tephras from Shiveluch volcano (SH1964, SH#28, and SH#34). Other regional Shiveluch tephras have overlapping glass chemistries but can be discerned and used as markers in cases where stratigraphic constraints are available. Three Kliuchevskoi tephras can be used as additional markers.

Our geochemical data permit a better characterization of a number of well-known regional tephras. In addition, we have characterized nine Shiveluch tephras that had not been recognized before in the proximal record. Our dataset presents a comprehensive record of the Shiveluch tephras deposited east of the volcano and provides new data for isopach maps and volume calculations. The first-ever analysis of pre-historic Kliuchevskoi tephras provides a record of large Kliuchevskoi eruptions with minimum bulk tephra volumes of ~0.20–0.25 km^3. The obtained data has also allowed us to estimate Holocene recurrence rate of heavy tephra falls (>0.5 cm) at the study area at 0.0025 yr-1 (1 event in 400 years on average).

In order to estimate the ages of tephra layers we combined a total of 223 ^{14}C dates in a single Bayesian framework, further improving the previously obtained age model for the proximal Shiveluch deposits (Ponomareva et al., 2015). This approach has permitted further refinement of tephra ages and estimates of ages for tephras which have not been directly dated.

Our study sites are to date the easternmost, fully analyzed sites in Kamchatka, which make their tephra sequences particularly relevant for tephra and cryptotephra research in the northwest Pacific, Bering Sea, Aleutian Islands, North America and potentially other distant localities. This study is a major step toward creating consistent Holocene tephrochronological framework and geochemical identification "tags" based on robust age models and glass geochemistry.

Acknowledgements

The research described in this paper was possible thanks to the U.S. National Science Foundation grant #0915131 to Ezra Zubrow and the Russian Foundation for Basic Research grant #15-05-02651 to Tatiana Pinegina. We acknowledge the GEOMAR Helmholtz Center funding for the electron microprobe analyses. Work on the manuscript was supported by the Russian Science Foundation grant #16-07-10035 and the Quaternary Research Center (University of Washington, USA). The authors thank Lilia Bazanova for a sample of AV_4 tephra, Mario Thöner, Nikita Mironov, and Olga Bergal-Kuvikas for their help with sample preparation and microprobe analysis, and Olga Uspenskaia for selection of macrofossils for ^{14}C dating in Izvilisty site.

Appendix A. Supplementary data

Supplementary data related to this article can be found at http://dx.doi.org/10.1016/j.quascirev.2017.04.031.

References

Adams, J., 1990. Paleoseismicity of the Cascadia subduction zone: evidence from turbidites off the Oregon-Washington margin. Tectonics 9 (4), 569–583.
Alloway, B.V., Lowe, D.J., Barrell, D.J., Newnham, R.M., Almond, P.C., Augustinus, P.C., Bertler, N.A., Carter, L., Litchfield, N.J., McGlone, M.S., Shulmeister, J., 2007. Towards a climate event stratigraphy for New Zealand over the past 30 000 years (NZ-INTIMATE project). J. Quat. Sci. 22 (1), 9–35.
Bazanova, L.I., Braitseva, O.A., Dirksen, O.V., Sulerzhitskii, L.D., Danhara, T., 2005. Ashfalls due to great Holocene eruptions along the Ust-Bolcheretsk-Petropavlovsk-Kamchatskii geotraverse: sources, chronology, rate of occurrence. Volcanol. Seismol. 6, 30–46 (In Russian with English abstract).
Blockley, S.P., Ramsey, C.B., Pyle, D.M., 2008. Improved age modelling and high-precision age estimates of late Quaternary tephras, for accurate palaeoclimate reconstruction. J. Volcanol. Geotherm. Res. 177 (1), 251–262.
Borchardt, G., Aruscavage, P., Millard, H.J., 1972. Correlation of the Bishop ash, a Pleistocene marker bed, using instrumental neutron activation analysis. J. Sediment. Petrol 42, 01–306.
Bourgeois, J., Pinegina, T.K., Ponomareva, V.V., Zaretskaia, N.E., 2006. Holocene tsunamis in the southwestern Bering Sea, Russian Far East and their tectonic implications. Geol. Soc. Am. Bull. 11 (3/4), 449–463. http://dx.doi.org/10.1130/B25726.1.
Braitseva, O.A., Sulerzhitsky, L.D., Litasova, S.N., Melekestsev, I.V., Ponomareva, V.V., 1993. Radiocarbon dating and tephrochronology in Kamchatka. Radiocarbon 35 (3), 463–476.
Braitseva, O.A., Melekestsev, I.V., Ponomareva, V.V., Sulerzhitsky, L.D., 1995. The ages of calderas, large explosive craters and active volcanoes in the Kuril-Kamchatka region, Russia. Bull. Volcanol. 57 (6), 383–402.
Braitseva, O.A., Melekestsev, I.V., Ponomareva, V.V., Kirianov, V. Yu., 1996. The caldera-forming eruption of Ksudach volcano about cal. AD 240, the greatest explosive event of our era in Kamchatka. J. Volcanol. Geotherm. Res. 70 (1–2), 49–66.
Braitseva, O.A., Ponomareva, V.V., Sulerzhitsky, L.D., Melekestsev, I.V., Bailey, J., 1997. Holocene key-marker tephra layers in Kamchatka, Russia. Quat. Res. 47 (2), 125–139.
Braitseva, O.A., Bazanova, L.I., Melekestsev, I.V., Sulerzhitsky, L.D., 1998. Largest Holocene eruptions of Avachinsky volcano, Kamchatka. Volcanol. Seismol. 20, 1–27.
Bronk Ramsey, C., 2009a. Bayesian analysis of radiocarbon dates. Radiocarbon 51 (1), 337–360.
Bronk Ramsey, C., 2009b. Dealing with outliers and offsets in radiocarbon dating. Radiocarbon 51 (3), 1023–1045.
Cherepanova, M.V., Lepskaya, E.V., Anderson, P., Lozhkin, A.V., 2013. Diatoms from Holocene sediments of the Nerpich'e Lake (Kamchatka). Issled. Vodn. Biol.

Resur. Kamchatki i severo-zapadnoi chasti Tihogo okeana 31, 45–61.
Davies, L.J., Jensen, B.J.L., Froese, D.G., Wallace, K.L., 2016. Late Pleistocene and Holocene tephrostratigraphy of interior Alaska and Yukon: key beds and chronologies over the past 30,000 years. Quat. Sci. Rev. 146, 28–53. http://dx.doi.org/10.1016/j.quascirev.2016.05.026.
Dirksen, O., van den Bogaard, C., Danhara, T., Diekmann, B., 2011. Tephrochronological investigation at Dvuh-yurtochnoe lake area, Kamchatka: numerous landslides and lake tsunami, and their environmental impacts. Quat. Int. 246 (1), 298–311.
Dirksen, V., Dirksen, O., Diekmann, B., 2013. Holocene vegetation dynamics in Kamchatka, Russian Far east. Rev. Palaeobot. Palynol. 190, 48–65.
Donoghue, S.L., Vallance, J., Smith, I.E., Stewart, R.B., 2007. Using geochemistry as a tool for correlating proximal andesitic tephra: case studies from Mt Rainier (USA) and Mt Ruapehu (New Zealand). J. Quat. Sci. 22 (4), 395–410.
Fedotov, S.A. (Ed.), 1984. Great Tolbachik Fissure Eruption, Kamchatka, 1975–1976. Nauka, Moscow, pp. 177–209 (In Russian).
Fedotov, S.A., Masurenkov, Yu.P. (Eds.), 1991. Active Volcanoes of Kamchatka, vol. 1. Nauka, Moscow, 302 pp.
Fontijn, K., Lachowycz, S.M., Rawson, H., Pyle, D.M., Mather, T.A., Naranjo, J.A., Moreno-Roa, H., 2014. Late Quaternary tephrostratigraphy of southern Chile and Argentina. Quat. Sci. Rev. 89, 70–84.
Fontijn, K., Rawson, H., Van Daele, M., Moernaut, J., Abarzúa, A.M., Heirman, K., Bertrand, S., Pyle, D.M., Mather, T.A., De Batist, M., Naranjo, J.A., 2016. Synchronisation of sedimentary records using tephra: a postglacial tephrochronological model for the Chilean Lake District. Quat. Sci. Rev. 137, 234–254.
Gehrels, M.J., Lowe, D.J., Hazell, Z.J., Newnham, R.M., 2006. A continuous 5300-yr Holocene cryptotephrostratigraphic record from northern New Zealand and implications for tephrochronology and volcanic hazard assessment. Holocene 16, 173–187.
Geist, E.L., Scholl, D.W., 1994. Large-scale deformation related to the collision of the Aleutian arc with Kamchatka. Tectonics 13, 538–560. http://dx.doi.org/10.1029/94TC00428.
Gill, J.B., 1981. Orogenic Andesites and Plate Tectonics. Springer, Berlin, 390 pp.
Goebel, T., Waters, M.R., Dikova, M., 2003. The archaeology of Ushki Lake, Kamchatka, and the Pleistocene peopling of the Americas. Science 301, 501–505.
Goebel, T., Slobodin, S.B., Waters, M.R., 2010. New dates from Ushki-1, Kamchatka, confirm 13,000 cal BP age for earliest Paleolithic occupation. J. Archaeol. Sci. 37 (10), 2640–2649.
Gorshkov, G.S., Dubik, Yu.M., 1970. Gigantic directed blast at Shiveluch volcano (Kamchatka). Bull. Volcanol. 34, 261–288.
Gudmundsdóttir, E.R., Larsen, G., Björck, S., Ingólfsson, Ó., Striberger, J., 2016. A new high-resolution Holocene tephra stratigraphy in eastern Iceland: improving the Icelandic and North Atlantic tephrochronology. Quat. Sci. Rev. 150, 234–249. http://dx.doi.org/10.1016/j.quascirev.2016.08.011.
Gusev, A.A., Ponomareva, V.V., Braitseva, O.A., Melekestsev, I.V., Sulerzhitsky, L.D., 2003. Great explosive eruptions on Kamchatka during the last 10,000 years: self-similar irregularity of the output of volcanic products. J. Geophys. Res. 108 (B2), 2126. http://dx.doi.org/10.1029/2001JB000312.
Hulse, E., Keeler, D., Zubrow, E., Korosec, G., Ponkratova, I., Curtis, C., 2011. Preliminary report on archaeological fieldwork in the Kamchatka region of Russia. Sibirica Interdiscip. J. Sib. Stud. 10 (1), 48–74.
Kozhurin, A., Acocella, V., Kyle, P.R., Lagmay, F.M., Melekestsev, I.V., Ponomareva, V.V., Rust, D., Tibaldi, A., Tunesi, A., Corazzato, C., Rovida, A., Sakharov, A., Tengonciang, A., Uy, H., 2006. Trenching active faults in Kamchatka, Russia: paleoseismological and tectonic implications. Tectonophysics 417, 285–304.
Kozhurin, A.I., Pinegina, T.K., 2011. Active faulting in the Kamchatsky Peninsula as evidence for the Kamchatka-Aleutian collision. In: 7th Biennial Workshp on Japan-Kamchatka-Alaska Subduction Processes: JKASP-2011, Petropavlovsk-kamchatsky, Russia, August 25–30, p. 125. www.kscnet.ru/ivs/slsecret/jkasp_2011/abstr/abs57.pdf.
Kozhurin, A.I., Pinegina, T.K., Ponomareva, V.V., Zelenin, E.A., Mikhailyukova, P.G., 2014. Rate of collisional deformation in Kamchatsky Peninsula, Kamchatka. Geotectonics 48 (2), 122–138.
Kutterolf, S., Freundt, A., Perez, W., Morz, T., Schacht, U., Wehrmann, H., Schmincke, H.U., 2008a. Pacific offshore record of plinian arc volcanism in Central America: 1. Along-arc correlations. Geochem. Geophys. Geosys. 9 http://dx.doi.org/10.1029/2007gc001631.
Kutterolf, S., Freundt, A., Perez, W., 2008b. Pacific offshore record of plinian arc volcanism in Central America: 2. Tephra volumes and erupted masses. Geochem. Geophys. Geosys. 9 http://dx.doi.org/10.1029/2007gc001791.
Kyle, Ph.R., Ponomareva, V.V., Rourke Schluep, R., 2011. Geochemical characterization of marker tephra layers from major Holocene eruptions in Kamchatka, Russia. Int. Geol. Rev. 53 (9), 1059–1097.
Larsen, G., 1981. Tephrochronology by microprobe glass analysis. In: Self, S., Sparks, R.S.J. (Eds.), Tephra Studies. D. Reidel, Dordrecht, pp. 95–102.
Lawson, I.T., Swindles, G.T., Plunkett, G., Greenberg, D., 2012. The spatial distribution of Holocene cryptotephras in north-west Europe since 7 ka: implications for understanding ash fall events from Icelandic eruptions. Quat. Sci. Rev. 41, 57–66. http://dx.doi.org/10.1016/j.quascirev.2012.02.018.
Legros, F., 2000. Minimum volume of a tephra fallout deposit estimated from a single isopach. J. Volcanol. Geotherm. Res. 96, 25–32.
Lowe, D.J., 2011. Tephrochronology and its application: a review. Quat. Geochronol. 6, 107–153.
MacInnes, B., Fitzhugh, B., Holman, D., 2014. Controlling for landform age when determining the settlement history of the Kuril Islands. Geoarchaeology 29 (3), 185–201. http://dx.doi.org/10.1002/gea.21473.
MacInnes, B., Kravchunovskaya, E., Pinegina, T., Bourgeois, J., 2016. Paleotsunamis from the central Kuril Islands segment of the Japan-Kuril-Kamchatka subduction zone. Quat. Res. 86 (1), 54–66.
Mackay, H., Hughes, P.D., Jensen, B.J., Langdon, P.G., Pyne-O'Donnell, S.D., Plunkett, G., Froese, D.G., Coulter, S., Gardner, J.E., 2016. A mid to late Holocene cryptotephra framework from eastern North America. Quat. Sci. Rev. 132, 101–113.
Melekestsev, I.V., Kurbatov, A.V., Pevzner, M.M., Sulerzhitsky, L.D., 1994. Prehistoric tsunamis and large earthquakes on the Kamchatsky Peninsula, Kamchatka, based on tephrochronological data. Volcanol. Seismol. 16, 449–459.
Moernaut, J., Daele, M.V., Heirman, K., Fontijn, K., Strasser, M., Pino, M., Urrutia, R., De Batist, M., 2014. Lacustrine turbidites as a tool for quantitative earthquake reconstruction: new evidence for a variable rupture mode in south central Chile. J. Geophys. Res. Solid Earth 119 (3), 1607–1633.
Nakamura, Y., 2016. Stratigraphy, distribution, and petrographic properties of Holocene tephras in Hokkaido, northern Japan. Quat. Int. 397, 52–62. http://dx.doi.org/10.1016/j.quaint.2015.07.056.
Óladóttir, B., Larsen, G., Sigmarsson, O., 2011. Holocene volcanic activity at Grímsvötn, Bárdarbunga and Kverkfjöll subglacial centres beneath Vatnajökull, Iceland. Bull. Volcanol. 73, 1187–1208. http://dx.doi.org/10.1007/s00445-011-0461-4.
Pedoja, K., Authemayou, C., Pinegina, T., Bourgeois, J., Nexer, M., Delcaillau, B., Regard, V., 2013. "Arc-continent collision" of the Aleutian-Komandorsky arc into Kamchatka: insight into Quaternary tectonic segmentation through Pleistocene marine terraces and morphometric analysis of fluvial drainage. Tectonics 32 (4), 827–842.
Pendea, I.F., Harmsen, H., Keeler, D., Zubrow, E.B., Korosec, G., Ruhl, E., Ponkratova, I., Hulse, E., 2016. Prehistoric human responses to volcanic tephra fall events in the Ust-Kamchatsk region, Kamchatka Peninsula (Kamchatsky Krai, Russian Federation) during the middle to late Holocene (6000–500 cal BP). Quat. Int. 394, 51–68. http://dx.doi.org/10.1016/j.quaint.2015.07.033.
Pendea, I.F., Ponomareva, V.V., Bourgeois, J., Zubrow, E.B.W., Portnyagin, M.V., Ponkratova, I., Harmsen, H., Korosec, G., 2017. Late glacial to Holocene paleoenvironmental change on the northwestern Pacific seaboard, Kamchatka Peninsula (Russia). Quat. Sci. Rev. 157, 14–28. http://dx.doi.org/10.1016/j.quascirev.2016.11.035.
Pevzner, M.M., Ponomareva, V.V., Melekestsev, I.V., 1998. Chernyi Yar – reference section of the Holocene ash markers at the northeastern coast of Kamchatka. Volcanol. Seismol. 19 (4), 389–406.
Pevzner, M.M., Ponomareva, V.V., Sulerzhitsky, L.D., 2006. Holocene soil-pyroclastic covers in the Central Kamchatka depression: age, structure, specifics of sedimentation. Volcanol. Seismol. 1, 24–38 (In Russian).
Pevzner, M.M., 2010. The northern boundary of volcanic activity of Kamchatka in Holocene. Bulletin of Kamchatka Regional association "Educational-scientific Center". Earth Sci. 1 (15), 117–144 [In Russian]. http://www.kscnet.ru/kraesc/2010/2010_15/ann11.html.
Pevzner, M.M., Tolstykh, M.L., Babansky, A.D., Kononkova, N.N., 2013. Reconstruction of the magmatic system in the Shiveluch volcanic massif as a result of large-scale collapses of its edifice in the late Pleistocene-early Holocene. Dokl. Earth Sci. 448 (1), 35–37.
Pinegina, T.K., Kozhurin, A.I., Ponomareva, V.V., 2012. Seismic and tsunami hazard for Ust'-Kamchatsk village, Kamchatka, based on paleoseismological data. Bull. Kamchatka Regional Assoc.. "Educational-scientific Center". Earth Sci. 1 (19), 138–159 [In Russian]. http://www.kscnet.ru/kraesc/2012/2012_19/2012_19_eng.html.
Pinegina, T., Ponomareva, V., Bourgeois, J., MacInnes, B., 2013a. Geomorphology is archaeological destiny: challenges in reconstructing habitations along the Kamchatka-Kuril Subduction Zone. In: 2013 GSA Annual Meeting in Denver.
Pinegina, T.K., Bourgeois, J., Kravchunovskaya, E.A., Lander, A.V., Arcos, M.E., Pedoja, K., MacInnes, B.T., 2013b. A nexus of plate interaction: vertical deformation of Holocene wave-built terraces on the Kamchatsky Peninsula (Kamchatka, Russia). Geol. Soc. Am. Bull. 125 (9–10), 1554–1568.
Pinegina, T.K., Kozhurin, A.I., Ponomareva, V.V., 2014. Active tectonics and geomorphology of the Kamchatsky Bay coast in Kamchatka. Russian J. Pac. Geol. 8 (1), 65–76.
Plunkett, G., Coulter, S.E., Ponomareva, V.V., Blaauw, M., Klimaschewski, A., Hammarlund, D., 2015. Distal tephrochronology in volcanic regions: challenges and insights from Kamchatkan lake sediments. Glob. Planet. Change 134, 26–40. http://dx.doi.org/10.1016/j.gloplacha.2015.04.006.
Ponomareva, V.V., Kyle, P.R., Pevzner, M.M., Sulerzhitsky, L.D., Hartman, M., 2007. Holocene eruptive history of Shiveluch volcano. Kamchatka Peninsula. In: Eichelberger, J., Gordeev, E., Kasahara, M., Izbekov, P., Lees, J. (Eds.), Volcanism and Subduction: the Kamchatka Region, American Geophysical Union Geophysical Monograph Series, vol. 172. AGU, Washington DC, pp. 263–282.
Ponomareva, V.V., Portnyagin, M.V., Melnikov, D.V., 2012. Composition of tephra from modern (2009-2011) eruptions of the Kamchatka and Kuril Islands volcanoes. Bulletin of Kamchatka Regional association "Educational-scientific Center". Earth Sci. 2 (20), 7–21 [In Russian]. http://www.kscnet.ru/kraesc/2012/2012_20/2012_20_eng.html.
Ponomareva, V., Portnyagin, M., Derkachev, A., Pendea, I.F., Bourgeois, J., Reimer, P.J., Garbe-Schönberg, D., Krasheninnikov, S., Nürnberg, D., 2013a. Early Holocene M~6 explosive eruption from Plosky volcanic massif (Kamchatka) and its tephra

as a link between terrestrial and marine paleoenvironmental records. Int. J. Earth Sci. 102 (6), 1673–1699. http://dx.doi.org/10.1007/s00531-013-0898-0.

Ponomareva, V., Portnyagin, M., Derkachev, A., Juschus, O., Garbe-Schönberg, D., Nürnberg, D., 2013b. Identification of a widespread Kamchatkan tephra: a middle Pleistocene tie-point between Arctic and Pacific paleoclimatic records. Geophys. Res. Lett. 40 (14), 3538–3543. http://dx.doi.org/10.1002/grl.50645.

Ponomareva, V., Portnyagin, M., Pevzner, M., Blaauw, M., Kyle, Ph., Derkachev, A., 2015. Tephra from andesitic Shiveluch volcano, Kamchatka, NW Pacific: Chronology of explosive eruptions and geochemical fingerprinting of volcanic glass. Int. J. Earth Sci. 104, 1459–1482. http://dx.doi.org/10.1007/s00531-015-1156-4.

Portnyagin, M., Ponomareva, V., Bindeman, I., Hauff, F., Krasheninnikov, S., Kuvikas, O., Mironov, N., Pletchova, A., van den Bogaard, C., Hoernle, K., 2009. Millennial variations of major and trace element and isotope compositions of Klyuchevskoy magmas, Kamchatka. Terra Nostra 1, 64–65.

Portnyagin, M., Mironov, N., Ponomareva, V., Bindeman, I., Hauff, F., Sobolev, A., Kayzar, T., Garbe-Schönberg, D., Hoernle, K., 2011. Arc Magmas from Slab to Eruption: the Case of Kliuchevskoy Volcano. Mineralogical Magazine. Abstracts of the 2011 Goldcshmidt Conference, Prague, p. 1661. http://www.minersoc.org.

Pouderoux, H., Proust, J.N., Lamarche, G., 2014. Submarine paleoseismology of the northern Hikurangi subduction margin of New Zealand as deduced from turbidite record since 16 ka. Quat. Sci. Rev. 84, 116–131.

Reimer, P.J., Bard, E., Bayliss, A., Beck, J.W., et al., 2013. IntCal13 and MARINE13 radiocarbon age calibration curves 0-50000 years calBP. Radiocarbon 55 (4). http://dx.doi.org/10.2458/azu_js_rc.55.16947.

Sawai, Y., Kamataki, T., Shishikura, M., Nasu, H., Okamura, Y., Satake, K., Thomson, K.H., Matsumoto, D., Fujii, Y., Komatsubara, J., Aung, T.T., 2009. A periodic recurrence of geologically recorded tsunamis during the past 5500 years in eastern Hokkaido, Japan. J. Geophys. Res. Solid Earth 114 (B1).

Shane, P., 2000. Tephrochronology: a New Zealand case study. Earth Sci.. Rev. 49 (1), 223–259.

Shane, P., 2005. Towards a comprehensive distal andesitic tephrostratigraphic framework for New Zealand based on eruptions from Egmont volcano. J. Quat. Sci. 20, 45–57.

Schindlbeck, J.C., Kutterolf, S., Freundt, A., Straub, S.M., Vannucchi, P., Alvarado, G.E., 2016. Late Cenozoic tephrostratigraphy offshore the southern Central American Volcanic Arc: 2. Implications for magma production rates and subduction erosion. Geochem. Geophys. Geosys. 17 (11), 4585–4604.

Schmid, M.M., Dugmore, A.J., Vésteinsson, O., Newton, A.J., 2016. Tephra isochrons and chronologies of colonisation. Quat. Geochronol. http://dx.doi.org/10.1016/j.quageo.2016.08.002.

Sherrod, B.L., Blakely, R.J., Lasher, J.P., Lamb, A., Mahan, S.A., Foit, F.F., Barnett, E.A., 2016. Active faulting on the Wallula fault zone within the Olympic-Wallowa lineament, Washington State, USA. Geol. Soc. Am. Bull. 313599-1.

Townsend, T., 1998. Paleoseismology of the Waverley Fault zone and implications for earthquake hazard in South Taranaki, New Zealand. N. Z. J. Geol. Geophys. 41 (4), 467–474.

Turner, R., Koehler, R.D., Briggs, R.W., Wesnousky, S.G., 2008. Paleoseismic and slip-rate observations along the Honey Lake fault zone, northeastern California, USA. Bull. Seismol. Soc. Am. 98 (4), 1730–1736.

Volynets, O.N., 1994. Geochemical types, petrology and genesis of Late Cenozoic volcanic rocks from the Kurile-Kamchatka island-arc system. Int. Geol. Rev. 36 (4), 373–405.

Volynets, O.N., Ponomareva, V.V., Babansky, A.D., 1997. Magnesian basalts of Shiveluch andesite volcano, Kamchatka. Petrology 5 (2), 183–196.

Volynets, O.N., Ponomareva, V.V., Braitseva, O.A., Melekestsev, I.V., Chen, Ch.H., 1999. Holocene eruptive history of Ksudach volcanic massif, South Kamchatka: evolution of a large magmatic chamber. J. Volcanol. Geotherm. Res. 91, 23–42.

Watson, E.J., Swindles, G.T., Lawson, I.T., Savov, I.P., 2016. Do peatlands or lakes provide the most comprehensive distal tephra records? Quat. Sci. Rev. 139, 110–128.

Zaretskaia, N., Ponomareva, V.V., Sulerzhitsky, L.D., Dirksen, O.V., 2001. Radiocarbon dating of the Kurile Lake caldera eruption (South Kamchatka, Russia). Geochronometria 20, 95–102.

Zharinov, N.A., Demyanchuk, Y.V., 2013. Large explosive eruptions of Shiveluch volcano, Kamchatka resulting in partial destruction of the extrusive dome (February 28, 2005 and October 27, 2010). J. Volcanol. Seismol 7 (2), 131–144.